NASA CONTRACTOR REPORT

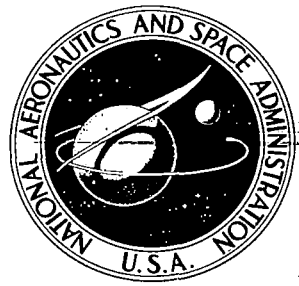

SUPERSONIC FLUTTER OF A THERMALLY STRESSED FLAT PLATE WITH EDGE STIFFENERS

by Harmohan Singh Sikand and Charles Libove

Prepared by
SYRACUSE UNIVERSITY
Syracuse, N. Y.
for Langley Research Center

NATIONAL AERONAUTICS AND SPACE ADMINISTRATION • WASHINGTON, D. C. • MAY 1970

SUPERSONIC FLUTTER OF A THERMALLY STRESSED FLAT PLATE WITH EDGE STIFFENERS*

By Harmohan Singh Sikand and Charles Libove

Issued by Originator as Report No. ME 1065-699

*This report was submitted as a thesis by the first author in partial fulfillment of the requirements for the Master of Mechanical Engineering Degree, October 1969.

Prepared under Grant No. NsG-385 by
SYRACUSE UNIVERSITY
Syracuse, N.Y.

for Langley Research Center

NATIONAL AERONAUTICS AND SPACE ADMINISTRATION

For sale by the Clearinghouse for Federal Scientific and Technical Information
Springfield, Virginia 22151 – CFSTI price $3.00

ABSTRACT

The effect of midplane stresses (uniform or non-uniform) due to prescribed temperature distributions over a simply supported isotropic rectangular plate with edge stiffeners on the flutter behavior of the plate when subjected to supersonic airflow over one surface is considered. The aerodynamic loading is assumed to be given by the two dimensional static aerodynamics or the Ackeret theory. In addition to the thermal and aerodynamic loading, the analysis includes external in-plane loadings distributed along each pair of opposite stiffeners.

All four stiffeners are assumed to be uniform and to possess finite axial stiffness and either zero or infinite bending stiffness in the plane of the plate. The plate edges are assumed to be integrally attached to the stiffeners along the centroidal axes of the stiffeners, and, in accordance with the simple support assumption, are assumed to provide infinite restraint against lateral deflection and no restraint against rotation.

The analysis is carried out in two parts. In the first part, the midplane stresses for the particular prescribed temperatures are evaluated, and in the second part the flutter behavior (or, more generally, the dynamic response) is determined. In evaluating the midplane stresses, Fourier series are used. In determining the flutter boundary Galerkin's technique is adopted.

The cases investigated are:

1) Rectangular plate with edge stiffeners of zero bending stiffness and finite axial stiffness, and a pillow-shaped temperature distribution (i.e., varying as half a sine wave in both directions).

2) Rectangular plate with edge stiffeners of infinite bending stiffness

and finite axial stiffness, and a pillow-shaped temperature distribution. 3) Rectangular plate with edge stiffeners of infinite bending stiffness and finite axial stiffness, with a temperature distribution discontinuous as follows: the plate temperature is constant at one value while the stiffener temperatures are constant at a different value.

Although the general analysis is as described above, numerical results were computed only for a square plate with all four stiffeners identical, and no external loading except for the aerodynamic loading. The numerical results show that the flutter boundary is significantly affected by the axial stiffness of the stiffeners, the flexural stiffness of the stiffeners and the type of temperature distribution.

ACKNOWLEDGMENT

This investigation was conducted at Syracuse University. The early phases of the investigation were supported by Grant Ns G-385 from the National Aeronautics and Space Administration. The remainder of the investigation, including the numerical work, was supported by Syracuse University. The authors are indebted to Dr. Kin N. Tong for his constructive suggestions. Thanks are also extended to Mrs. Virginia Nortman for typing this work.

TABLE OF CONTENTS

LIST OF FIGURES

INTRODUCTION

One of the problems to be considered in the design of modern high-speed aerospace vehicles is the flutter of external skin panels in the supersonic regions of flight. Flutter is an aeroelastic, self-excited vibration in which the external source of energy is the airstream. A large number of parameters influence this phenomenon. The purpose of the present paper is to investigate the effect of one of these parameters, namely, thermally induced midplane stresses.

A prior investigation of this kind was made by Schaeffer and Heard (ref.1)who studied the supersonic flutter behavior of a flat rectangular plate with uniform edge loading in both directions and a non-uniform temperature distribution which varied parabolically in both directions over the plate but was constant through the thickness. The edges of the plate were assumed to be simply supported, but otherwise free of any external constraint.

The present investigation is similar to Schaeffer and Heard's but introduces different conditions with regard to external constraint. The edges are still considered to be simply supported (i.e., to have zero lateral deflection and zero normal bending moment), but are assumed to be integrally attached to stiffeners of finite axial stiffness along their centroidal axes. With regard to the flexural stiffness of these stiffeners for bending in the plane of the plate, two limiting cases are considered: zero flexural stiffness and infinite flexural stiffness. The latter case corresponds to the situation in which the edges are held straight or nearly straight because of the continuity between the plate and neighboring plates across the stiffeners; the former corresponds to the case in which there is little or no surrounding material beyond the edge stiffeners.

The simple support assumption implies that the edge stiffeners are considered to have negligible torsional stiffness.

The main difference between the present investigations and Schaeffer and Heard's lies in the edge conditions as described above. However, there are two minor differences between the present paper and reference 1 with regard to external loading and temperature distribution: Whereas reference 1 considers a *uniform* biaxial external loading, the present work considers a biaxial loading which need only be symmetric about each center line of the plate. And while reference 1 employs a parabolic temperature distribution, the present analysis assumes a sinusoidal one. In addition, for the case of flexurally rigid stiffeners only, the present paper also considers a discontinuous temperature distribution with the stiffener temperature constant at one value and the plate temperature constant at a different value. As in reference 1, the temperature is assumed in all cases not to vary through the thickness.

The analysis consists of two parts: the evaluation of the midplane stresses due to the temperature distribution as well as external loading, and the flutter analysis proper, using these midplane stresses. For the evaluation of the midplane stresses the techniques of references 2 and 3 are mainly employed, which are based on double Fourier series. The flutter analysis is executed by means of the Galerkin method in the manner of reference 1. As in reference 1, the aerodynamic loading is assumed to be given by the two dimensional static aerodynamics or Ackeret theory. For the special case of the plate with flexurally rigid edge stiffeners and discontinuous temperature distribution (stiffener temperature constant at one value, plate temperature constant at a different value), it was found that the midplane stress problem could be solved by elementary considerations,

leading to a homogenous state of stress in the plate, and then the solution to the flutter problem could be extracted from the results of reference 1 by merely redefining certain parameters.

Based on the general analysis, numerical results are computed for the case of a square plate with all stiffeners identical and no external loading. For the sinusoidal (hereinafter called "pillow-shaped") temperature distribution calculations were made for both the zero and infinite flexural stiffness cases. For the discontinuous temperature distribution numerical results are given only for infinite flexural stiffness case.

The numerical results for these three cases are compared with each other. Those for the pillow-shaped temperature distribution are compared with those of Schaeffer and Heard in order to indicate the effect of the edge stiffeners. As is to be expected, for a given amplitude of temperature the presence of the stiffeners raises the general magnitude of the in-plane thermal compressive stresses and thereby lowers the flutter boundary. For the same reason, the fluexurally rigid stiffeners lead to a greater lowering of the flutter boundary than do the perfectly flexible stiffeners; and the discontinuous temperature distribution leads to a greater lowering of the flutter boundary than does the pillow-shaped temperature, in the case of flexurally rigid stiffeners.

DETAILED DESCRIPTION OF STRUCTURE AND LOADING

The configuration of plate and stiffeners is shown schematically in Figure 1. The plate is rectangular and flat, of length a, width b, and thickness h. Any point on the plate is defined by its x and y coordinates in the Cartesian reference frame whose axes coincide with two adjacent edges of the plate, as shown in Figure 1. The structure is symmetric about each of its two center lines. Thus the cross-sectional areas of the stiffeners located along $x = 0$ and $x = a$ are both denoted by the same symbol A_1, and the cross-sectional areas of the stiffeners at $y = 0$ and $y = b$ are both denoted by A_3. It is assumed that the stiffener axes coincide with the plate edges.

The plate is homogeneous, elastic, and isotropic, with Young's modulus E, and Poisson's ratio ν, and coefficient of thermal expansion α. The stiffeners are assumed to have the same Young's modulus and the same thermal expansion coefficients as the plate.

The temperature distributions $T(x,y)$ are also taken symmetric about each center line of the structure. The pillow-shaped temperature distribution is defined by

$$T(x,y) = \theta \sin \frac{P\pi x}{a} \sin \frac{Q\pi y}{b} \tag{1}$$

where P and Q are both equal to unity* and θ is the value of the temperature at the center of the plate. The discontinuous temperature

---

*By superimposing terms of this type, with P and Q having different combinations of odd values and the θ in each term being a function of P and Q, one can approximate any symmetric temperature distribution. The stresses due to such a temperature distribution can then be obtained by superimposing the stresses due to the individual terms. It is for this reason that the subsequent analysis is carried through with P and Q left as symbols rather than being replaced by their numerical value of prime interest, unity.

distribution is defined by $T = 0$ along the stiffeners and $T = \theta$ = constant over the plate. In both cases the temperature $T(x,y)$ is measured with respect to some datum temperature distribution for which the structure is assumed to be stress free in the absense of external loads.

The external edge loadings are also taken to be symmetric about each center line of the plate. For the case of perfectly flexible stiffeners these loadings are assumed to be nonuniform as shown in Figure 1. $N_1(y)$ denotes the force per unit length (positive for tension) acting on the stiffeners at $x = 0$ and $x = a$, $N_3(x)$ the force per unit length on the other pair of stiffeners.

For the case of flexurally rigid stiffeners it is, of course, immaterial, as far as the plate stresses and flutter behavior are concerned, what the actual distribution of the external loading is like. It is only the resultant force on each edge that is significant in influencing the plate behavior. In the present paper these resultant forces are denoted by T_1 (positive for tension) for the stiffeners at $x = 0$ and $x = a$, and by T_3 for the stiffeners at $y = 0$ and $y = b$, and they are assumed to act at the center of each stiffener as shown in Figure 2.

The air is assumed to be flowing over one surface of the plate in the x-direction (see Fig. 1) at a supersonic Mach number of M. When the plate is perfectly flat the air stream produces no lateral force upon it. When the plate deflects, however, the air stream exerts lateral pressures which are assumed to be given by the linearized, static, two dimensional supersonic aerodynamic theory or Ackeret theory. According to this theory, which is said to be accurate for Mach number greater than 1.3 (ref. 4), the aerodynamic tension "ℓ" on the plate surface due to an air stream flowing in the positive x-direction is given by

$$\ell = - \frac{2q^*}{\sqrt{M^2-1}} \frac{\partial w}{\partial x}$$

where

$q^* = 1/2\ \rho V^2$

V = velocity of air stream

ρ = mass density of air

$w(x,y,t)$ = lateral plate deflection

t = time

and the air is flowing over that surface of the plate which is on the positive w side. The minus sign in the formula indicates that for these conditions a positive slope will produce a local pressure (i.e., negative aerodynamic tension).

The partial differential equation governing the motion of the plate for small lateral deflections, and which will form the basis of the subsequent flutter analysis is

$$D\nabla^4 w - N_x w_{,xx} - 2N_{xy} w_{,xy} - N_y w_{,yy} + \mu h w_{,tt} = \ell \qquad (2)$$

where

μ = plate density (mass per unit volume)

$D = \frac{Eh^3}{12(1-\nu^2)}$ = plate flexural stiffness

and commas indicate partial differentiation with respect to the subscripted co-ordinates.

This plate partial differential equation is equation (217) of reference 5 with the lateral loading term q in that equation expressed in terms of the aerodynamic tension ℓ and the inertia loading due to

plate motion. It must be solved subject to the following boundary conditions of simple support:

$$w(o,y,t) = w(a,y,t) = w(x,o,t) = w(x,b,t) = 0$$

$$w_{,xx}(o,y,t) = w_{,xx}(a,y,t) = w_{,yy}(x,o,t) = w_{,yy}(x,b,t) = 0 \tag{3}$$

EVALUATION OF PLATE STRESSES

This section will describe the evaluation of the inplane plate stress resultants required as prerequisites for the determination of the flutter behavior. These stresses are shown schematically in Figure 3; they are denoted by N_x and N_y for the normal stress resultants and by N_{xy} for the shear stress resultant and have the dimensions of force per unit length. Figure 3 also shows the notation for the internal stiffener cross-sectional tensions, namely $P_1(y)$ for the $x = 0$ and a stiffeners, $P_3(x)$ for the $y = 0$ and b stiffeners. $P_1(y)$ and $P_3(x)$ have the dimensions of force.

Case 1: Pillow-Shaped Temperature Distribution, Perfectly Flexible Stiffeners.

For the case of perfectly flexible stiffeners, reference 2 treats a greatly generalized version of the stress problem considered here. In reference 2 the plate may be orthotropic or isotropic, the structure, loading, and temperature distribution are not necessarily symmetric, and the external loading may include stiffener end tensions and shear flows acting along the outer periphery of the stiffeners.

Therefore the plate stresses required for the present investigation can be obtained from the equations of reference 2 by specializing those equations in accordance with the more restricted nature of the present configuration, that is by omitting the external shear flows and stiffener end tensions, incorporating the symmetry of the structure, loading and temperature distribution, and expressing the orthotropic elastic constants in terms of the isotropic ones, E and ν.

The derivations in reference 2 are based upon the plate compatibility equation, the stiffener axial equilibrium equations, the condition of compatibility of strain between each stiffener and the plate edge to which it is attached, the boundary conditions of prescribed loading, and the expansion of all known and unknown quantities in terms of Fourier series. It is left to the interested reader to see reference 2 for these derivations. Here only the specialized results of reference 2 needed for the present purpose will be given. The results for the stiffener stresses, although not needed for the flutter analysis of the plate, will be given as additional information of interest.

In order to use the results of reference 2 we require, not the temperature distribution itself, but the thermal strains that it would produce if every infinitesimal element of the structure were free to undergo its thermal expansion unrestrained. These thermal strains are shown schematically in Figure 4. For the plate they will be denoted by $e_x(x,y)$ and $e_y(x,y)$ in the x and y directions respectively. For the stiffeners at $x = 0$ and a they will be denoted by $e_1(y)$, and for the stiffeners at $y = 0$ and b by $e_3(x)$. Under the present assumptions of isotropy and uniformity of material properties and a pillow-shaped temperature distribution, these strains are

$$e_x = e_y = \alpha\theta \sin \frac{P\pi x}{a} \sin \frac{Q\pi y}{b}$$

$$e_1 = e_3 = 0 \tag{4}$$

Reference 2 further requires that certain functions of these thermal strains be expressed in the form of Fourier series as follows:

$$e_1(y) - e_y(o,y) = \sum_{n\ odd}^{\infty} T_n' \sin \frac{n\pi y}{b} \quad \text{for} \quad 0 < y < b$$

$$e_3(x) - e_x(x,o) = \sum_{m\ odd}^{\infty} T_m''' \sin \frac{m\pi x}{a} \quad \text{for} \quad 0 < x < a \tag{5}$$

$$\frac{\partial^2 e_y}{\partial x^2} + \frac{\partial^2 e_x}{\partial y^2} = \sum_{m,n\ odd}^{\infty} \sum T_{mn} \sin \frac{m\pi x}{a} \sin \frac{n\pi y}{b} \quad \text{for} \quad \begin{matrix} 0 < x < a \\ 0 < y < b \end{matrix}$$

In the present case, with e_x, e_y, e_1, e_3 as given by equation (4), the above Fourier coefficients are readily seen to be

$$T_n' = T_m''' = 0$$

$$T_{mn} = \begin{cases} -\alpha\theta\pi^2 \left(\frac{P^2}{a^2} + \frac{Q^2}{b^2}\right) & \text{for} \quad m = P \quad \text{and} \quad n = Q \\ 0 & \text{otherwise} \end{cases} \tag{6}$$

Similarly, reference 2 requires that the external edge loadings be known in the form of Fourier series as follows:

$$N_1(y) = \sum_{n\ odd}^{\infty} B_n' \sin \frac{n\pi y}{b} \quad \text{for} \quad 0 < y < b$$

$$N_3(x) = \sum_{m\ odd}^{\infty} B_m''' \sin \frac{m\pi x}{a} \quad \text{for} \quad 0 < x < a \tag{7}$$

For the case of uniform edge loading ($N_1(y)$ = constant = N_1, $N_3(x)$ = constant = N_3) the Fourier coefficients in these series would be given by $B_n' = 4N_1/(n\pi)$ and $B_m''' = 4N_3/(m\pi)$.

With the above Fourier coefficients known, reference 2 then yields the following series for computing the plate stress resultants and stiffener tensions in the case where structure, loading, and temperature distribution are symmetric about each center line of the plate:

$$N_x = \sum_{m,n}^{M} \sum_{\text{odd}}^{N} g_{mn} \sin \frac{m\pi x}{a} \sin \frac{n\pi y}{b} \qquad \text{for} \quad 0 < x < a, \; 0 < y < b$$

$$N_y = \sum_{m,n}^{M} \sum_{\text{odd}}^{N} c_{mn} \sin \frac{m\pi x}{a} \sin \frac{n\pi y}{b}$$

$$N_{xy} = -\sum_{m,n}^{M} \sum_{\text{odd}}^{N} j_{mn} \cos \frac{m\pi x}{a} \cos \frac{n\pi y}{b} \qquad \text{for} \quad 0 \leq x \leq a, \; 0 \leq y \leq b$$

$$N_x\Big)_{y=0 \text{ or } b} = \sum_{m \text{ odd}}^{M} g_m' \sin \frac{m\pi x}{a} \qquad \text{for} \quad 0 < x < a \qquad (8)$$

$$N_y\Big)_{x=0 \text{ or } a} = \sum_{n \text{ odd}}^{N} c_n' \sin \frac{n\pi y}{b} \qquad \text{for} \quad 0 < y < b$$

$$P_1(y) = \sum_{n \text{ odd}}^{N} s_n' \sin \frac{n\pi y}{b} \qquad \text{for} \quad 0 < y < b$$

$$P_3(x) = \sum_{m \text{ odd}}^{M} s_m''' \sin \frac{m\pi x}{a} \qquad \text{for} \quad 0 < x < a$$

(In reference 2, which considered the possibility of stiffener end tensions as part of the external loading, the above series for $P_1(y)$ and $P_3(x)$

were not valid at the end points, $y = 0,b$ and $x = 0, a$ respectively, because they yield identically zero values there. Consequently the regions of validity for these series are indicated above as open regions. In the present case, however, since stiffener end loads are absent the values of $P_1(y)$ and $P_3(x)$ are actually zero at the end points; and the above series for $P_1(y)$ and $P_3(x)$ in the present case are therefore also valid in the closed regions $0 \leq y \leq b$ and $0 \leq x \leq a$, respectively.)

The Fourier coefficients appearing in the above series can be evaluated in terms of the known Fourier coefficients $T_n'(=0)$, $T_m'''(=0)$, T_{mn}, B_n', B_m'''. The procedure is as follows:

First the g_m' and c_n' are determined by solving the following system of simultaneous equations (specialized form of eqs. (B61'') and (B63'') of ref. 2):

$$\bar{c}_n' \left[A_1 E + \frac{4}{a} \sum_{m \text{ odd}}^{M} \left(\frac{m\pi}{a}\right)^2 \frac{1}{E_{mn}}\right] = R_n' - \frac{4}{b}\left(\frac{n\pi}{b}\right)^2 \sum_{m \text{ odd}}^{M} \frac{\bar{g}_m'}{E_{mn}}$$

$$n = 1,3,\ldots, N$$

$$\bar{g}_m' \left[A_3 E + \frac{4}{b} \sum_{n \text{ odd}}^{N} \left(\frac{n\pi}{b}\right)^2 \frac{1}{E_{mn}}\right] = R_m''' - \frac{4}{a}\left(\frac{m\pi}{a}\right)^2 \sum_{n \text{ odd}}^{N} \frac{\bar{c}_n'}{E_{mn}} \tag{9}$$

$$m = 1,3,\ldots, M$$

where

$$\bar{c}_n' = \frac{c_n'}{Eh} \cdot \frac{n\pi}{b}$$

$$\bar{g}_m' = \frac{g_m'}{Eh} \frac{m\pi}{a} \tag{9a}$$

$$E_{mn} = \frac{1}{Eh}\left[\left(\frac{m\pi}{a}\right)^2 + \left(\frac{n\pi}{b}\right)^2\right]^2$$

$$R_n' = A_1 E \frac{n\pi}{b} \left(\frac{\nu}{Eh} B_n' + T_n'\right) - \sum_{m\ odd}^{M} K_{mn}$$

$$R_m''' = A_3 E \frac{m\pi}{a} \left(\frac{\nu}{Eh} B_m''' + T_m'''\right) - \sum_{n\ odd}^{N} K_{mn} \qquad (9a)$$

$$K_{mn} = \frac{1}{E_{mn}} \left\{ \frac{mn\pi^2}{ab} T_{mn} - \frac{4}{b} \left(\frac{m\pi}{a}\right)^3 \frac{B_m'''}{Eh} - \frac{4}{a} \left(\frac{n\pi}{b}\right)^3 \frac{B_n'}{Eh} \right\}$$

The symbols M and N which appear as upper summation limits in equations (8) and which also determine the number of simultaneous equations in equation (9), are positive odd integers whose values should be taken as large as possible for the sake of accuracy (up to the point whose round off errors may begin to offset accuracy).

With the c_n' and g_m' computed through equations (9), the remaining Fourier coefficients in the series (8) can be readily obtained from the following formulas:

$$g_{mn} = -\frac{4}{b} \left(\frac{n\pi}{b}\right) \left(\frac{a}{m\pi}\right)^2 B_m''' + \left(\frac{n\pi}{b}\right)^2 A_{mn}$$

$$c_{mn} = -\frac{4}{a} \left(\frac{m\pi}{a}\right) \left(\frac{b}{n\pi}\right)^2 B_n' + \left(\frac{m\pi}{a}\right)^2 A_{mn}$$

$$j_{mn} = \frac{4}{b} \left(\frac{a}{m\pi}\right) B_m''' + \frac{4}{a} \left(\frac{b}{n\pi}\right) B_n' - \left(\frac{m\pi}{a}\right) \left(\frac{n\pi}{b}\right) A_{mn} \qquad (10)$$

$$s_n' = \frac{A_1}{h} \left(- T_n' Eh + c_n' - \nu B_n'\right)$$

$$s_m''' = \frac{A_3}{h} \left(- T_m''' Eh + g_m' - \nu B_m'''\right)$$

where

$$A_{mn} = \left[\left(\frac{m\pi}{a}\right)^2 + \left(\frac{n\pi}{b}\right)^2\right]^{-2} \left\{ T_{mn} Eh + \frac{4}{a} \frac{m\pi}{a} c_n' + \frac{4}{b} \left(\frac{n\pi}{b}\right) g_m' \right.$$

$$\left. + \frac{4}{a} \frac{m\pi}{a} \left(\frac{b}{n\pi}\right)^2 \left[\left(\frac{m\pi}{a}\right)^2 + 2 \left(\frac{n\pi}{b}\right)^2\right] B_n' + \frac{4}{b} \frac{n\pi}{b} \left(\frac{a}{m\pi}\right)^2 \left[\left(\frac{n\pi}{b}\right)^2 + 2 \left(\frac{m\pi}{a}\right)^2\right] B_m''' \right\}$$

The simultaneous equations (9) can be considerably simplified if one deals with the special case of a square plate (a=b) with structure, loading and temperature symmetrical not only about the center lines but also about the diagonals, i.e., $A_1 = A_3$, $B_i' = B_i'''$, $T_i' = T_i'''$, $T_{ij} = T_{ji}$. The corresponding symmetry that should result in the plate and stiffener stresses is described by the following equations:

$$N_x(\xi,\eta) = N_y(\eta,\xi)$$

$$N_{xy}(\xi,\eta) = N_{xy}(\eta,\xi)$$

$$P_1(\eta) = P_3(\eta)$$

In order for this symmetry to be reflected in the results of the numerical calculations one chooses M and N equal. Then equations (9) reduce to

$$\bar{g}_i' = \bar{c}_i' \qquad (i = 1,3, \ldots, M) \tag{11}$$

$$\bar{c}_n' \left[A_1 E + \frac{4}{a} \sum_{m \text{ odd}}^{M} \left(\frac{m\pi}{a}\right)^2 \frac{1}{E_{mn}}\right] = R_n' - \frac{4}{a}\left(\frac{n\pi}{a}\right)^2 \sum_{m \text{ odd}}^{M} \frac{\bar{c}_m'}{E_{mn}}$$

$$(n = 1,3, \ldots, M) \tag{12}$$

Thus for this highly symmetric case it is necessary to solve only equations (12) for the $\bar{c}_n'$. Then equations (11) immediately give the $\bar{g}_m'$.

In order to provide stresses for use in connection with the subsequent numerical flutter calculations equations (12) were further specialized to the case of no external loads ($B_i' = B_i''' = 0$). Using equations (6) for the T_n', T_m''' and T_{mn}, and substituting (9a) for the R_n', equations (12) can then be put into the following form most suitable for calculations:

$$C_n \left[\frac{1}{\lambda_i} + \sum_{m \text{ odd}}^{M} \frac{m^2}{(m^2+n^2)^2}\right] + n^2 \sum_{m \text{ odd}}^{M} \frac{C_m}{(m^2+n^2)^2} = \delta_{nQ} \frac{\pi P}{4(P^2+Q^2)} \tag{13}$$

$$n = 1,3. \ . \ ., M$$

where

$$C_n = \frac{c_n'}{\alpha\theta Eh} \tag{14}$$

$$\lambda_1 = \frac{4ah}{\pi^2 A_1}$$

and δ_{nQ} is Kronecker's delta. The dimensionless parameter λ_1 is seen to be a measure of the ratio of plate cross-sectional area to stiffener cross-sectional area. It is of interest to note that for $\lambda_1 \to 0$, this system of equations reduces to the especially simply form:

$$C_n = \delta_{nQ} \lambda_1 \pi P/[4(P^2+Q^2)]$$

With the C_n known, equation (10) then gives the following Fourier series coefficients for this case:

$$g_{mn} = \alpha\theta Eh \left\{ \frac{4n^2}{\pi(m^2+n^2)^2} [m C_n + n C_m] - \frac{Q^2}{(P^2+Q^2)} \delta_{mP} \delta_{nQ} \right\}$$

$$c_{mn} = \alpha\theta Eh \left\{ \frac{4m^2}{\pi(m^2+n^2)^2} [m C_n + n C_m] - \frac{P^2}{(P^2+Q^2)} \delta_{mP} \delta_{nQ} \right\} \tag{15}$$

$$j_{mn} = \alpha\theta Eh \left\{ - \frac{4mn}{\pi(m^2+n^2)^2} [m C_n + n C_m] + \frac{PQ}{(P^2+Q^2)} \delta_{mP} \delta_{nQ} \right\}$$

$$s_n' = A_1 E\alpha\theta C_n$$

Equations (13) were solved simultaneously for the case of $\lambda_1 = 1$, using $M = 59$ and $P = Q = 1$. The solution was by means of the Gauss-Seidel iterative procedure. The resulting values of C_n are given in

column (a) of Table 1. The corresponding stresses, as given by equations (8) in conjunction with equations (15), are plotted in Figure 6 in dimensionless form. Because of the symmetry, it suffices to show results for only one quadrant of the structure.

Case 2: Pillow-Shaped Temperature Distribution, Flexurally Rigid Stiffeners

The stress analysis problem considered here is a special case of the problem treated in Appendix E of reference 3, which deals with an edge-stiffened rectangular plate with each stiffener bent and held into a prescribed shape. In the present case the prescribed shape is one of zero curvature. Reference 3 furthermore permits the plate to be orthotropic or isotropic and does not require the structure, loading and temperature distribution to possess symmetry. In addition the external loading of reference 3 includes not only the resultant tensions T_1 and T_3 considered here (see Fig. 2), but also includes resultant external moments in the plane of the plate, stiffener end tensions, and shear flows acting along the outer periphery of the stiffeners. Therefore the stress analysis needed for the present purpose can be obtained by adapting the analysis of reference 3 to the more specialized characteristics of the present configuration.

In the previous case (perfectly flexible stiffeners) any external normal loading $N_1(y)$ and $N_3(x)$ was transmitted to the plate edges through the stiffeners without any change. Thus the coefficients B_n' and B_m''', which defined this external loading through equations (7), also defined the normal stress resultants acting along the plate edge. In the present case (stiffeners rigidly held to a prescribed shape) the distributions of normal stress along the plate edges are unknown. If $N_1(y)$ and $N_3(x)$ (eq. 7) now denote not the external loading but

these distributions of normal stress resultant along the plate edges then the B_n' and B_m''' represent two systems of unknowns for the present problem. Additional unknowns in the present problem are the mutual forces which the stiffeners exert upon each other at their junctions. Despite the larger number of unknowns in the present problem as compared with that of Case 1, the problem is solvable by virtue of additional imposed conditions on the present one, namely the requirements that a) the curvature of a plate edge be compatible at every point with the prescribed curvature of the attached stiffener, and b) that each stiffener be in equilibrium under the action of the external loading, the normal stress exerted on it by the plate, and the end reactions upon it exerted by the adjacent stiffeners. The detailed derivation of the stress analysis for this case will not be given here. The interested reader is referred to reference 3 for this derivation. Here only those results of reference 3 pertinent to the present flutter problem will be given. The results for the stiffener tensions will again be given as additional information of interest.

Reference 3 requires the same given basic information on thermal strains as in Case 1, namely equations (4), (5), and (6). In addition it requires that two additional thermal-strain quantities be known in the form of Fourier series, to wit:

$$\left.\frac{\partial e_y}{\partial x}\right)_{x=0} = \sum_{n\ \text{odd}}^{N} V_n' \sin\frac{n\pi y}{b} \qquad (0 < y < b)$$

$$\left.\frac{\partial e_x}{\partial y}\right)_{y=0} = \sum_{m\ \text{odd}}^{M} V_m''' \sin\frac{m\pi x}{a} \qquad (0 < x < a) \tag{16}$$

and it requires that the prescribed curvatures of the edge stiffeners be known in the form of the following series:

$$\left.\frac{\partial^2 u}{\partial y^2}\right)_{x=0} = \sum_{n\ \text{odd}}^{N} K_n' \sin\frac{n\pi y}{b} \qquad (0 < y < b)$$

$$\left.\frac{\partial^2 v}{\partial x^2}\right)_{y=0} = \sum_{m\ \text{odd}}^{M} K_m''' \sin\frac{m\pi x}{a} \qquad (0 < x < a) \tag{17}$$

where $u(x,y)$ and $v(x,y)$ are the x-wise and y-wise components of displacement. In the present case, since the stiffeners are held straight the Fourier coefficients K_n' and K_m''' will be zero, and they will therefore not appear in the subsequent equations. In view of equation (4) for the pillow-shaped temperature distributions, V_n' and V_m''' become

$$V_n' = \alpha\theta \frac{P\pi}{a} \delta_{nQ}$$

$$V_m''' = \alpha\theta \frac{Q\pi}{b} \delta_{nP} \tag{18}$$

The results for the plate stress resultants and stiffener tensions can again be given in the form of equations (8) augmented by the following equations:

$$N_x(o,y) = N_x(a,y) = \sum_{n\ \text{odd}}^{N} B_n' \sin\frac{n\pi y}{b} \qquad (0 < y < b)$$

$$N_y(x,o) = N_y(x,b) = \sum_{m\ \text{odd}}^{M} B_m''' \sin\frac{m\pi x}{a} \qquad (0 < x < a)$$

$$P_1(0+) = P_1(b-) = \frac{T_3}{2} - \sum_{m\ \text{odd}}^{M} \frac{a}{m\pi} B_m''' \tag{19}$$

$$P_3(0+) = P_3(a-) = \frac{T_1}{2} - \sum_{n\ \text{odd}}^{N} \frac{b}{n\pi} B_n'$$

The Fourier coefficients appearing in the above and in equations (8) are determined by first solving the following system of simultaneous equations for the B_n', B_m''', $\bar{c}_n'$ and $\bar{g}_m'$ (adapted from eqs. (E23) to (E30) of ref. 3):

$$B_n' \left[\gamma_n^{(1)} - \gamma_n^{(2)}\right] = \delta_n' - \sum_{m\ \text{odd}}^{M} 2\,\Lambda_{mn}'\,B_m''' + \sum_{m\ \text{odd}}^{M} 2\,\mu_{mn}'\,\bar{g}_m' + \sum_{m\ \text{odd}}^{M} 2\,\nu_{mn}'\,\bar{c}_n' \qquad (n = 1,3,\ldots N)$$

$$B_m''' \left[\Gamma_m^{(1)} - \Gamma_m^{(2)}\right] = \delta_m''' - \sum_{n\ \text{odd}}^{N} 2\,\Lambda_{mn}''\,B_n' + \sum_{n\ \text{odd}}^{N} 2\,\mu_{mn}''\,\bar{c}_n' + \sum_{n\ \text{odd}}^{N} 2\,\nu_{mn}''\,\bar{g}_m' \qquad (m = 1,3,\ldots M) \qquad (20)$$

$$\bar{c}_n' \left[\alpha_1(n) - \beta_1(n)\right] = S_n' + \sum_{m\ \text{odd}}^{M} 2\,\pi_{mn}\,B_m''' + B_n'\left(\gamma_n' - \gamma_n''\right) - \frac{4}{b}\left(\frac{n\pi}{b}\right)^2 \sum_{m\ \text{odd}}^{M} \frac{\bar{g}_m'}{E_{mn}} \qquad (n = 1,3,\ldots N)$$

$$\bar{g}_m' \left[\alpha_3(m) - \beta_2(m)\right] = S_m''' + \sum_{n\ \text{odd}}^{N} 2\,H_{mn}\,B_n' + B_m'''\left(\Gamma_m' - \Gamma_m''\right) - \frac{4}{a}\left(\frac{m\pi}{a}\right)^2 \sum_{n\ \text{odd}}^{N} \frac{\bar{c}_n'}{E_{mn}} \qquad (m = 1,3,\ldots M)$$

where

$$\bar{c}_n' = c_n' \frac{1}{Eh} \left(\frac{n\pi}{b}\right)$$

$$\bar{g}_m' = g_m' \frac{1}{Eh} \left(\frac{m\pi}{a}\right)$$

$$[\gamma_n^{(1)} - \gamma_n^{(2)}] = -\frac{4}{a} \left(\frac{n}{b}\right)^2 \frac{1}{Eh} \sum_{m \text{ odd}}^{M} \bar{E}_{mn} \left[(2 + \nu) \left(\frac{n}{b}\right)^2 + \left(\frac{m}{a}\right)^2\right]$$

$$[\Gamma_m^{(1)} - \Gamma_m^{(2)}] = -\frac{4}{b} \left(\frac{m}{a}\right)^2 \frac{1}{Eh} \sum_{n \text{ odd}}^{N} \bar{E}_{mn} \left[(2 + \nu)\left(\frac{m}{a}\right)^2 + \left(\frac{n}{b}\right)^2\right]$$

$$\delta_n' = -K_n' - V_n' - \sum_{m \text{ odd}}^{M} \bar{E}_{mn} \left\{\frac{T_{mn}}{\pi} \left(\frac{m}{a}\right) \left[(2 + \nu)\left(\frac{n}{b}\right)^2 + \left(\frac{m}{a}\right)^2\right]\right\}$$

$$\delta_m''' = -K_m''' - V_m''' - \sum_{n \text{ odd}}^{N} \bar{E}_{mn} \left\{\frac{T_{mn}}{\pi} \left(\frac{n}{b}\right) \left[(2 + \nu)\left(\frac{m}{a}\right)^2 + \left(\frac{n}{b}\right)^2\right]\right\}$$

$$\Lambda_{mn}' = \frac{2}{b} \left(\frac{n}{b}\right)\left(\frac{m}{a}\right) \left(\frac{1}{Eh}\right) \bar{E}_{mn} \left[\left(\frac{n}{b}\right)^2 - \nu \left(\frac{m}{a}\right)^2\right]$$

$$\Lambda_{mn}'' = \frac{2}{a} \left(\frac{m}{a}\right)\left(\frac{n}{b}\right) \frac{1}{Eh} \bar{E}_{mn} \left[\left(\frac{m}{a}\right)^2 - \nu \left(\frac{n}{b}\right)^2\right]$$

$$\mu_{mn}' = -\frac{2}{b} \left(\frac{n}{b}\right) \frac{1}{\pi} \bar{E}_{mn} \left[(2 + \nu)\left(\frac{n}{b}\right)^2 + \left(\frac{m}{a}\right)^2\right]$$

$$\mu_{mn}'' = -\frac{2}{a} \left(\frac{m}{a}\right) \frac{1}{\pi} \bar{E}_{mn} \left[(2 + \nu)\left(\frac{m}{a}\right)^2 + \left(\frac{n}{b}\right)^2\right]$$

$$\nu_{mn}' = \frac{2}{a} \left(\frac{n}{b}\right) \frac{1}{\pi} \bar{E}_{mn} \left[\left(\frac{n}{b}\right)^2 - \nu\left(\frac{m}{a}\right)^2\right]$$

$$\nu_{mn}'' = \frac{2}{b} \left(\frac{m}{a}\right) \frac{1}{\pi} \bar{E}_{mn} \left[\left(\frac{m}{a}\right)^2 - \nu\left(\frac{n}{b}\right)^2\right]$$

$$[\alpha_1(n) - \beta_1(n)] = A_1 E + \frac{4}{a} \sum_{m\ odd}^{M} (\frac{m\pi}{a})^2 / E_{mn}$$

$$[\alpha_3(m) - \beta_2(m)] = A_3 E + \frac{4}{b} \sum_{n\ odd}^{N} (\frac{n\pi}{b})^2 / E_{mn}$$

$$S_n' = A_1 E\ (\frac{n\pi}{b})\ T_n' - \sum_{m\ odd}^{M} \frac{1}{E_{mn}}\ \frac{mn\pi^2}{ab}\ T_{mn} + \frac{2T_3}{b}$$

$$S_m''' = A_3 E\ (\frac{m\pi}{a})\ T_m''' - \sum_{n\ odd}^{N} \frac{1}{E_{mn}}\ \frac{mn\pi^2}{ab}\ T_{mn} + \frac{2T_1}{a} \qquad (21)$$

$$[\gamma_n' - \gamma_n''] = A_1 E\ (\frac{n\pi}{b})\ \frac{\nu}{Eh} + \frac{4}{a}\ (\frac{n}{b})^3\ \frac{1}{\pi} \sum_{m\ odd}^{M} \bar{E}_{mn}$$

$$[\Gamma_m' - \Gamma_m''] = A_3 E\ (\frac{m\pi}{a})\ \frac{\nu}{Eh} + \frac{4}{b}\ (\frac{m}{a})^3\ \frac{1}{\pi} \sum_{n\ odd}^{N} \bar{E}_{mn}$$

$$\pi_{mn} = \frac{2}{b}\ (\frac{m\pi}{a})\ [\frac{1}{E_{mn}}\ (\frac{m\pi}{a})^2\ \frac{1}{Eh} - (\frac{a}{m\pi})^2\ ]$$

$$H_{mn} = \frac{2}{a}\ (\frac{n\pi}{b})\ [\frac{1}{E_{mn}}\ (\frac{n\pi}{b})^2\ \frac{1}{Eh} - (\frac{b}{n\pi})^2\ ]$$

$$\bar{E}_{mn} = [(\frac{m}{a})^2 + (\frac{n}{b})^2]^{-2}$$

(As in the previous case, M and N are selected odd integers; by increasing M and N increasing accuracy is obtained, subject to the limitations due to round-off errors.) With the B_n', B_m''', c_n' ($= \bar{c}_n'\ Ehb/(n\pi)$), g_m' ($= \bar{g}_m'\ Eha/(m\pi)$) computed through equations (20),

we have thus evaluated the Fourier coefficients needed in equation (19). To obtain the remaining required Fourier coefficients, namely those in equations (8), equations (10) of the previous case are used.

The simultaneous equations (20) can be considerably simplified if one deals with the special case of a square structure (a=b) with symmetry not only about the center lines but also about the diagonals ($T_1 = T_3$, $A_1 = A_3$, $T_i' = T_i'''$, $T_{ij} = T_{ji}$). In order for this physical symmetry to be reflected in the mathematical solution, it is necessary to pick M and N equal. Then equations (20) reduces to

$$\bar{g}_i' = \bar{c}_i' \qquad (i = 1,3,\ldots,M) \quad (22)$$

$$B_i''' = B_i'$$

$$B_n'[\gamma_n^{(1)} - \gamma_n^{(2)}] = \delta_n' - \sum_{m\ \text{odd}}^{M} 2\,\Lambda_{mn}'\,B_m' + \sum_{m\ \text{odd}}^{M} 2\,\mu_{mn}'\,\bar{c}_m' + \sum_{m\ \text{odd}}^{M} 2\,\nu_{mn}'\,\bar{c}_n' \qquad (n = 1,3,\ldots,M) \quad (23)$$

$$\bar{c}_n'[\alpha_1(n) - \beta_1(n)] = S_n' + \sum_{m\ \text{odd}}^{M} 2\,\pi_{mn}\,B_m' + B_n'\,(\gamma_n' - \gamma_n'') - \frac{4}{b}\left(\frac{n\pi}{b}\right)^2 \sum_{m\ \text{odd}}^{M} \frac{\bar{c}_m'}{E_{mn}} \qquad (n = 1,3,\ldots,M)$$

Thus for this highly symmetric case it is necessary to solve only system (23) for the $\bar{c}_n'$ and B_n'. Then equations (22) gives $\bar{g}_m'$ and B_m'''.

For the later numerical flutter calculation, equations (23) were further specialized to the case of no external load ($T_1 = T_3 = 0$) and temperature distributions as described by equations (1), (4) and (6). The resulting form of equations (23), taking into account equations (21), is

$$\left\{\frac{(1-\nu)}{2} - 2n^2 \sum_{p\ \text{odd}}^{M} \frac{[p^2 + (2+\nu)n^2]}{[p^2 + n^2]^2}\right\} B_n = \delta_{nQ} \frac{P\pi}{2} \left\{\frac{[P^2 + (2+\nu)Q^2]}{[P^2 + Q^2]} - 1\right\}$$

$$- 2n \sum_{p\ \text{odd}}^{M} \frac{p[p^2 + (2+\nu)n^2]}{[p^2 + n^2]^2} C_p + 2n^2 C_n \sum_{p\ \text{odd}}^{M} \frac{[n^2 - \nu p^2]}{[p^2 + n^2]^2}$$

$$- 2n \sum_{p\ \text{odd}}^{M} \frac{p[n^2 - \nu p^2]}{[p^2 + n^2]^2} B_p (1 - \delta_{np})$$

$$(n = 1,3,\ldots,M)$$

$$\left\{n[1 + \lambda_1 \sum_{p\ \text{odd}}^{M} \frac{p^2}{[p^2 + n^2]^2}] + \frac{\lambda_1}{4n}\right\} C_n = \delta_{nQ} \frac{\pi\lambda_1}{4} \frac{PQ}{[P^2 + Q^2]}$$

$$+ [\nu n + \lambda_1 n^3 \sum_{p\ \text{odd}}^{M} \frac{1}{[p^2 + n^2]^2}] B_n + \lambda_1 \sum_{p\ \text{odd}}^{M} [\frac{p^3}{[p^2 + n^2]^2} - \frac{1}{p}] B_p$$

$$- \lambda_1 n^2 \sum_{p\ \text{odd}}^{M} \frac{p(1-\delta_{pn})}{[p^2 + n^2]^2} C_p$$

$$(n = 1,3,\ldots,M) \qquad (24)$$

where

$$B_n = \frac{B_n'}{\alpha\theta Eh}$$

$$C_n = \frac{C_n'}{\alpha\theta Eh} \qquad (25)$$

$$\lambda_1 = \frac{4\ ah}{\pi^2 A_1}$$

The reduced form of equations (10) corresponding to this specialization is:

$$g_{mn} = \alpha\theta Eh \left\{ \frac{4n^2}{\pi[m^2 + n^2]^2} [mC_n + nC_m] + \frac{4m}{\pi} \frac{[m^2 + 2n^2]}{[m^2 + n^2]^2} B_n \right.$$

$$\left. + \frac{4n}{\pi m^2} \left[\frac{n^2(n^2 + 2m^2)}{[m^2 + n^2]^2} - 1\right] B_m - \frac{Q^2}{[P^2 + Q^2]} \delta_{mP} \delta_{nQ} \right\}$$

$$c_{mn} = \alpha\theta Eh \left\{ \frac{4m^2}{\pi[m^2 + n^2]^2} [mC_n + nC_m] + \frac{4n}{\pi} \frac{[n^2 + 2m^2]}{[m^2 + n^2]^2} B_m \right.$$

$$\left. + \frac{4m}{\pi n^2} \left[\frac{m^2(m^2 + 2n^2)}{[m^2 + n^2]^2} - 1\right] B_n - \frac{P^2}{[P^2 + Q^2]} \delta_{mP} \delta_{nQ} \right\}$$

$$j_{mn} = \alpha\theta Eh \left\{ \frac{PQ}{[P^2 + Q^2]} \delta_{mP} \delta_{nQ} - \frac{4m^2 n}{\pi[m^2 + n^2]^2} C_n - \frac{4mn^2}{\pi[m^2 + n^2]^2} C_m \right.$$

$$\left. + \frac{4m^3}{\pi[m^2 + n^2]^2} B_m + \frac{4n^3}{\pi[m^2 + n^2]^2} B_n \right\}$$

$$s_n' = A_1 E\alpha\theta [C_n - \nu B_n] \qquad (26)$$

where the B_n and C_n are computed from equations(24).

Equations (24) were solved simultaneously for the case $\lambda_1 = 1$, using $M = 59^*$ and $P = Q = 1$. The Gauss-Seidel iterative procedure was

---

*M = N = 59 was found to lead to sufficiently accurate results in reference 3.

employed. The resulting values of C_n and B_n are given in columns (b) and (c) of Table 1. The corresponding stresses, as given by equations (8) and (19) in conjunction with equations (26), are plotted in Figure 7 in dimensionless form. Because of the symmetry the stresses are given for only one quadrant of the structure.

Case 3: Discontinuous Temperature Distribution, Flexurally Rigid Stiffeners.

Here we consider the case of perfectly rigid stiffeners with stiffener temperatures constant at the value zero, plate temperature constant at the value θ, and the structure and loading symmetrical about each center line (Fig. 2).

To determine the stress resultants, we start by assuming that a state of homogeneous biaxial normal stress exists in the plate, and then show that this assumption leads to a solution which satisfies all the requirements of equilibrium and compatible deformations for the elements of the structure.

Figure 5 shows the free-body diagrams of the stiffeners and plate on the assumption that the plate stress resultants are

$$\begin{aligned} N_x\,(x,y) &= \text{constant} = N_x \\ N_y\,(x,y) &= \text{constant} = N_y \\ N_{xy}\,(x,y) &= 0 \end{aligned} \tag{27}$$

The plate and each element of it is obviously in equilibrium under this stress field. The unknown stress resultants N_x and N_y also act on the stiffener by virtue of Newton's third law. Since the stiffeners are flexurally rigid, mutual internal reactions are to be expected at the stiffener junctions. These reactions act as pairs of equal and opposite

forces, one appearing as a shear force at the end of a stiffener and the other an equal tension force at the end of the adjacent stiffener. The forces labeled $1/2\ (T_1 - N_x\ b)$ at the point (a,b) in Figure 5 are a typical pair of such mutual internal reactions. The magnitude $1/2\ (T_1 - N_x\ b)$ was arrived at by considering the equilibrium of the stiffener at $x = a$.

With the end reactions so obtained, equilibrium is completely satisfied for all elements of Figure 5. It remains to determine the two unknowns N_x and N_y. These will be determined from the condition that the (uniform) elongation of any stiffener and the (uniform) elongation of the plate edge to which it is attached must be equal. Writing this condition for the edge $x = 0$ or a, one obtains

$$\frac{1/2(T_3 - N_y\ a)b}{A_1 E} = \left[\frac{N_y - \nu N_x}{Eh} + \alpha\theta\right]b \tag{28}$$

Similarly for the edge $y = o$ or b,

$$\frac{1/2(T_1 - N_x\ b)a}{A_3 E} = \left[\frac{N_x - \nu N_y}{Eh} + \alpha\theta\right]a \tag{29}$$

Solving simultaneously for N_x and N_y yields

$$N_x = \frac{\left[1 + \frac{ah}{2A_1}\right]\left[\frac{T_1 h}{2A_3} - \alpha\theta Eh\right] + \nu\left(\frac{T_3 h}{2A_1} - \alpha\theta Eh\right)}{\left[1 + \frac{ah}{2A_1}\right]\left[1 + \frac{bh}{2A_3}\right] - \nu^2}$$

$$N_y = \frac{\left[1 + \frac{bh}{2A_3}\right]\left[\frac{T_3 h}{2A_1} - \alpha\theta Eh\right] + \nu\left(\frac{T_1 h}{2A_3} - \alpha\theta Eh\right)}{\left[1 + \frac{ah}{2A_1}\right]\left[1 + \frac{bh}{2A_3}\right] - \nu^2} \tag{30}$$

These values of N_x and N_y insure overall compatibility of elongation for a stiffener and the plate edge to which it is attached. Since the stiffener and plate strains are uniform, point-wise compatibility is also insured. Finally, the edges of the plate obviously remain straight under the stress distribution (27), i.e., compatible with the flexural rigidity of the stiffeners. We have thus arrived at a stress distribution for the structure that satisfies all the requirements of equilibrium and compatibility and which therefore must be the correct one.

In the subsequent flutter analysis the special case of a square structure (a=b), with symmetry about the diagonals as well as the center lines ($A_1 = A_3$), and with no external load ($T_1 = T_3 = 0$) will be considered. For this case, equations (30) become

$$N_x = N_y = - \frac{\alpha\theta Eh}{[(1-\nu) + \frac{ah}{2A_1}]} \tag{31}$$

FLUTTER ANALYSIS

Having evaluated the mid-plane stresses, we can now turn to the problem of studying the possible kinds of transverse motion of the plate in the presence of these stresses and the airstream, and determining those circumstances under which the motion can be characterized as flutter. The analytical procedure to be employed is the same for cases 1 and 2 (pillow-shaped temperature distribution with perfectly flexible or flexurally rigid stiffeners), and therefore these two cases are discussed together in a single section below. Case 3 (discontinuous temperature distribution with flexurally rigid stiffeners) is discussed in a separate section.

Cases 1 and 2: Pillow-Shaped Temperature Distribution, Perfectly Flexible or Flexurally Rigid Stiffeners.

The differential equation and boundary conditions have already been presented in equations (2) and (3). Here we will seek solutions of these equations in the form

$$w(x,y,t) = \left\{ \sum_{p=1}^{\infty} \sum_{q=1}^{\infty} a_{pq} \sin \frac{p\pi x}{a} \sin \frac{q\pi y}{b} \right\} e^{i\omega t} \qquad (32)$$

where a_{pq} and ω are as yet undetermined constants and $i = \sqrt{-1}$. Equation (32) obviously satisfies all the boundary conditions (eq. 3). Since the differential equation (2) is linear any combination of solutions of the above form will also be a solution.

The form of solution assumed in equation (32), namely the product of a spatial function and $e^{i\omega t}$, has been employed by Schaeffer and Heard (ref. 1) as well as by others (ref. 5 and 6). In Appendix B we attempt to show that there is no loss of generality in assuming solutions of the above form.

Substituting equation (32), along with expressions (eq. 8) for the stress resultants, into equation (2), and for computational purposes replacing the infinite upper summation limits of equation (32) by finite values R and S respectively, we obtain:

$$\sum_{p=1}^{R}\sum_{q=1}^{S} a_{pq} \sin\frac{p\pi x}{a} \sin\frac{q\pi y}{b} \left[\left(\frac{p}{a}\right)^2 + \left(\frac{q}{b}\right)^2\right]^2$$

$$+ \frac{1}{D\pi^2} \sum_{m,n\ \text{odd}}^{M,N} \sum_{p=1}^{R}\sum_{q=1}^{S} a_{pq} \left\{\left(\frac{p}{a}\right)^2 g_{mn} + \left(\frac{q}{b}\right)^2 c_{mn}\right\} \sin\frac{m\pi x}{a} \sin\frac{p\pi x}{a} \sin\frac{n\pi y}{b} \sin\frac{q\pi y}{b}$$

$$+ \frac{2}{D\pi^2} \sum_{m,n\ \text{odd}}^{M,N} \sum_{p=1}^{R}\sum_{q=1}^{S} \frac{pq}{ab} a_{pq} j_{mn} \cos\frac{m\pi x}{a} \cos\frac{p\pi x}{a} \cos\frac{n\pi y}{b} \cos\frac{q\pi y}{b}$$

$$- \frac{K^2}{a^4} \sum_{p=1}^{R}\sum_{q=1}^{S} a_{pq} \sin\frac{p\pi x}{a} \sin\frac{q\pi y}{b} + \frac{\lambda}{a^4\pi^3} \sum_{p=1}^{R}\sum_{q=1}^{S} p\, a_{pq} \cos\frac{p\pi x}{a} \sin\frac{q\pi y}{b} = 0 \qquad (33)$$

where

λ = aerodynamic pressure parameter = $\dfrac{2q^* a^3}{D\sqrt{M^2-1}}$

K^2 = frequency parameter = $\dfrac{\mu h\, a^4}{D\, \pi^4}\, \omega^2$

and the common factor $e^{i\omega t}$ has been cancelled. The procedures for determining the g_{mn}, c_{mn}, and j_{mn} which appear in the above equation have already been described in the previous section.

Equation (33) will now be solved for the a_{pq}'s and ω (or K^2) by Galerkin's technique (ref. 7). To that end we write the following system of equations:

$$\int_0^a \int_0^b H(x,y) \sin\frac{r\pi x}{a} \sin\frac{s\pi y}{b}\, dy\, dx = 0 \qquad (34)$$

$$r = 1,2,\ldots,R$$

$$s = 1,2,\ldots,S$$

where $H(x,y)$ stands for the entire left-hand side of equation (33). Substituting for $H(x,y)$ and carrying out the integrations indicated in equation (34) one obtains the following system of equations for the a_{pq}'s

$$\left\{\left[\left(\frac{r}{a}\right)^2 + \left(\frac{s}{b}\right)^2\right]^2 - \frac{K^2}{a^4}\right\} a_{rs} + \frac{16}{D\pi^4} \sum_{m,n}^{M} \sum_{\text{odd}}^{N} \sum_{p=1}^{R} \sum_{q=1}^{S} pqrs \; a_{pq} \left\{ \begin{matrix} (p+r) \\ (q+s) \end{matrix} \right\} = \text{even}$$

$$\left. \frac{4mn\left[\left(\frac{p}{a}\right)^2 g_{mn} + \left(\frac{q}{b}\right)^2 c_{mn}\right] + \frac{2}{ab} j_{mn} (r^2 - m^2 - p^2)(s^2 - n^2 - q^2)}{[(m-p+r)(m-p-r)(m+p+r)(m+p-r)][(n-q+s)(n-q-s)(n+q+s)(n+q-s)]} \right\}$$

$$+ \frac{2\lambda}{a^4\pi^4} \sum_{\substack{p=1 \\ p \neq r}}^{R} rp \; a_{ps} \frac{[1 - (-1)^{p+r}]}{[r^2 - p^2]} = 0 \qquad (35)$$

For $r = 1,2,\ldots,R$

$s = 1,2,\ldots,S$

The above equation represents R times S linear, homogeneous, algebraic equations which the unknown amplitude coefficients a_{rs} and the frequency parameter K^2 must satisfy. The reader is reminded that the influence of any applied loads and temperature distribution appears implicitly in the coefficients g_{mn}, c_{mn} and j_{mn}; and the influence of the airstream is in the aerodynamic pressure parameter λ.

These equations always have the trivial solution $a_{rs} = 0$ for all combinations of r and s. This solution represents no motion whatsoever of the plate (see eq. 32) and is therefore of no interest. Of interest are solutions for the a_{rs} and K^2 such that some of the a_{rs} are not zero. Such solutions can exist only for those values of K^2 that make

the determinant Δ of the coefficients of the a_{rs} in equations (35) vanish. Thus one arrives at an eigenvalue problem. For any given airstream (λ), loads and temperature (i.e., known g_{mn}, c_{mn}, j_{mn}), one must solve for those values of K^2 which satisfy the equation

$$\Delta = 0$$

Each such K^2 leads to two values of ω, and each value of ω leads to a solution (motion) of the form of equation (32). The value of ω itself determines the temporal form of that solution; the spatial form of the solution is determined by substituting the particular value of K^2 into equations (35) and using those equations to compute the relative magnitudes of the a_{rs}. The general motion of the plate is a superposition of the component motions (each of the form of eq. 32) corresponding to all the individual values of ω satisfying the equation $\Delta = 0$. The amount of each component present in any particular motion of the plate depends, of-course, on the initial conditions whereby the motion was started. In this investigation we will not be concerned with any specific initial conditions. Instead, imagining that all kinds of initial conditions are conceivable, we will concern ourselves with the values of K^2 (ω) and the temporal behavior of the component motions implied by these values.

Any particular value of K^2 may be (a) real and negative, (b) zero, (c) real and positive, or (d) complex. The corresponding values of ω and the implications regarding the temporal behavior of the component motions of the plate are as follows: (a) a real and negative K^2 gives two purely imaginary values of ω, one positive and one negative. It is seen from equation (32) that the positive imaginary value of ω leads to a component motion that is of the non-oscillatory subsident type; i.e., $e^{i\omega t}$ becomes a negative exponential. On the other hand, the negative

imaginary value of ω leads to a positive exponential and hence represents a non-oscillatory divergent component of motion. The case K^2 real and negative will therefore be characterized by its detrimental characteristic, namely *divergence*.

(b) A zero value of K^2 leads to zero values of ω, which eliminates time from equation (32) and therefore represents *static buckling*.

(c) K^2 real and positive leads to two real values of ω, both of which represent component motions of the form of simple harmonic motion, i.e., *ordinary vibration*.

(d) K^2 complex will lead to two complex values of ω, one the negative of the other. One of these values of ω will have a positive imaginary part, and the corresponding component of motion will therefore be an oscillatory one with subsiding amplitude. However, the other value of ω will have a negative imaginary part and will lead to an oscillatory motion with ever-increasing amplitude. This type of motion is what we call *flutter*. The case K^2 complex will be characterized as *flutter*, since this is its more detrimental consequence.

Since the equation $\Delta = 0$ has more than one root (i.e., more than one value of K^2 satisfying it), several of the above types of component motions can exist simultaneously. If any one of them is of the flutter type (case d), the motion will be described as *flutter*. If none is of flutter type, but one is of the divergence type (case a), the motion will be characterized as *divergence*. If none is of the flutter or divergence type, but one is of the static buckling type (case b), the behavior will be described as *static buckling*. Finally, if none of the component motions is of the flutter, divergence or static buckling type (i.e., all of the roots are real and positive as discussed in case c), then the motion is a

a superposition of ordinary vibrations and it will be described as *ordinary vibration.*

If one is concerned only with determining the "flutter boundary", i.e., those physical conditions which represent a transition from a non-flutter behavior to a flutter behavior, it is evident from the above that this boundary is defined by any one of the K^2 values passing from real to complex as the physical conditions change. The equation $\Delta = 0$, with Δ expanded as a polynomial in K^2, has real coefficients; therefore any complex roots for K^2 come in complex conjugate pairs. Consequently, assuming that the roots vary continuously with a continuous variation in the physical conditions, one can determine the transition from non-flutter to flutter behavior by seeking those physical conditions at which two real values of K^2 become real and equal.

One final point is worth mentioning before we pass to a specific case. By examining equations (35) it is evident that these equations can be separated into two distinct groups: those equations corresponding to $s = 1,3,5. \ . \ .$ contain only those a_{rs} with second subscript odd; and those equations resulting from $s = 2,4,6, \ . \ . \ .$ contain only those a_{rs} with second subscript even. Consequently the equation $\Delta = 0$ can be factored into two equations;

$$\Delta' = 0 \qquad \Delta'' = 0$$

where Δ' is the determinant of the coefficients of the a_{rs} with second subscript odd, and Δ'' the determinant formed from the coefficients of those a_{rs} with second subscript even. The matrices leading to Δ' and Δ'' are each of smaller order than the matrix leading to Δ. The roots of the equation $\Delta' = 0$ will in general lead to motions which are symmetric

about the center line of the plate parallel to the airstream; on the other hand the equation $\Delta'' = 0$ in general leads to motions which are anti-symmetric about this center line and for which this center line forms a node.

Equations (35) apply to the general case of a pillow-shaped temperature distribution and a rectangular structure with symmetry of structure and loading about each center line, and with perfectly flexible or flexurally rigid stiffeners. Numerical results will be presented for the special case considered earlier in connection with the stress analysis problem, i.e., a square structure with no external load and symmetry about the diagonals as well as the center lines. Equations (35) are specialized to this case by setting $a=b$ and by substituting for g_{mn}, c_{mn}, j_{mn} the following expressions:

$$\begin{aligned} g_{mn} &= \alpha\theta Eh\, G_{mn} \\ c_{mn} &= \alpha\theta Eh\, C_{mn} \\ j_{mn} &= \alpha\theta Eh\, J_{mn} \end{aligned} \tag{36}$$

where G_{mn}, C_{mn}, J_{mn} are defined, implicitly, by equations (15) for the case of perfectly flexible stiffeners or by equations (26) for the case of flexurally rigid stiffeners. With these substitutions made, and introducing a thermal-load parameter ψ defined by

$$\psi = \frac{\alpha\theta Eh\, a^2}{D\pi^2} = \alpha\theta\left(\frac{a}{h}\right)^2 \frac{12(1-\nu^2)}{\pi^2} \quad , \tag{37}$$

one obtains the following reduced form of equations (35):

$$[(r^2 + s^2)^2 - K^2]\, a_{rs} + \frac{16\psi}{\pi^2} \sum_{\substack{p=1 \\ p+r = \text{even} \\ q+s = \text{even}}}^{R} \sum_{q=1}^{S} a_{pq}\, pqrs \left\{ \sum_{\substack{m,n \\ \text{odd}}}^{M} \sum^{N} \frac{4mn[p^2 G_{mn} + q^2 C_{mn}] + 2 J_{mn} (r^2 - m^2 - p^2)(s^2 - n^2 - q^2)}{[(m-p+r)(m-p-r)(m+p+r)(m+p-r)][(n-q+s)(n-q-s)(n+q+s)(n+q-s)]} \right\}$$

$$+ \frac{2\lambda}{\pi^4} \sum_{\substack{p=1 \\ p \neq r}}^{R} a_{ps}\, rp \frac{[1 - (-1)^{p+r}]}{(r^2 - p^2)} = 0 \qquad (38)$$

for $r = 1,2,\ldots,R$

$s = 1,2,\ldots,S$

For a square plate it seems plausible to assume that those spatial modes which are symmetrical about the center lines parallel to the airstream will govern; i.e., detrimental behavior (divergence, static buckling or flutter) will occur at lower air speeds or lower temperature in these modes than in the anti-symmetric modes.* Therefore only those equations of equation (38) corresponding to odd values of s will be used in the computations. Taking six terms in the flow direction ($r = 1,2,\ldots 6$) and three terms in the cross-flow direction ($s = 1,3,5$), with $M = N = 59$, $P = Q = 1$, and $\lambda_1 = 1$, one obtains the eighteen simultaneous equations shown in Table 2 for the case of perfectly flexible stiffeners and in Table 3 for the case of flexurally rigid stiffeners. (To obtain these equations it was first necessary to solve the stress analysis problem by the procedure already described for cases 1 and 2 in the previous section.)

---

*Results supporting this contention may be found in reference 1.

The eigenvalues (K^2) of these matrices were determined by J. G. F. Francis' Unitary-Triangular or QR Transformation Method (ref.8) for selected constant value of the thermal-load parameter ψ and varying values of the aerodynamic-pressure parameter λ .

Figure 8 shows a typical set of results obtained by this method. Plotted in Figure 8 are the real parts of the eigenvalues K^2 versus the aerodynamic pressure parameter λ for the case of perfectly flexible stiffeners and $\psi = 12$. It is seen that the plot is a series of loops, the number depending on the values of R and S. In the case of $R = 6$ and $S = 5$, there are nine loops, corresponding to eighteen eigenvalues; however, only three loops are shown for the sake of simplicity in Figure 8. Each loop has a stem at the peak (e.g. point c') representing the value of $\lambda = \lambda_{critical}$ at which two real roots become equal and above which they become complex conjugates. Figure 8 shows all of the types of values of K^2 discussed earlier. The point labeled "a" and all such points to the left of the λ axis correspond to divergence (case a: K^2 real and negative). The point labeled "b" corresponds to static buckling (case b: K^2 zero). All points labeled "c", i.e., all points to the right of the λ axis and below the peaks of respective loops, correspond to ordinary vibration (case c: K^2 real and positive). All points, such as "d", which lie on the stems emanating from the peaks correspond to flutter (case d: K^2 complex). A peak point such as "c' " represents the transition from a non flutter to a flutter character of a pair of roots.

The first loop has the lowest peak and therefore determines the lowest flutter speed. Being furthest to the left it also determines the first occurrence of static buckling or divergence. Thus the first loop

alone is of practical significance for the purposes of this investigation, and for this reason the upper portions of the other loops were not determined precisely. Figure 9(a) shows how these first loops vary with ψ for the case of perfectly flexible stiffeners, and Figure 10(a) does the same for the case of flexurally rigid stiffeners. It is seen that for sufficiently small ψ there is no intersection with the λ axis, i.e., neither static buckling nor divergence can occur. As ψ increases the peak (flutter speed) is lowered, and eventually the loop does intersect the λ-axis, implying that static buckling and divergence can occur.

Figures 9(b) and 10(b) summarize the important information implied in Figures 9(a) and 10(a). The curve labeled $\lambda = \lambda_{cr}$ shows how the ordinate λ of the peak point c' of the first loop varies with ψ. This curve represents the boundary between those combinations of λ and ψ (above the curve) producing flutter and those combinations of λ and ψ (below the curve) which do not produce flutter. The non-flutter region (below the curve labeled $\lambda = \lambda_{cr}$) is divided into sub-regions, one representing those combinations of λ and ψ which are capable of supporting only ordinary vibrations, and two others representing those combinations of λ and ψ which are capable of supporting a divergent type of behavior. The curve labeled "static buckling" is the locus in the $\lambda - \psi$ plane of points such as "b" where the first loop intersects the λ axis; it constitutes a boundary between the sub-regions.

Case 3: Discontinuous Temperature Distribution, Flexurally Rigid Stiffeners

The stress analysis for this case showed that the state of stress in the plate was one of homogeneous biaxial normal stress (see eq. 30). The flutter analysis for this situation was done in reference 1 (where it corresponds to their case $\psi = 0$), and therefore some numerical results for this can be obtained from those of reference 1 by properly re-labeling the parameters. Such numerical results will be presented for the case of a square plate (a=b) with four identical stiffeners and no external load. For this case equation (31) gives:

$$N_x = N_y = - \frac{\alpha\theta Eh}{[(1-\nu) + \frac{ah}{2A_1}]} \tag{39}$$

The top curve of Figure 6 of reference 1 gives λ_{cr} for this case as a function of the external load parameters R_{x_o} and R_{y_o}, which are defined by

$$R_{x_o} = - \frac{N_x a^2}{\pi^2 D}$$

$$R_{y_o} = - \frac{N_y a^2}{\pi^2 D} \tag{40}$$

For N_x and N_y as given by equation (31), R_{x_o} and R_{y_o} become

$$R_{x_o} = k_{y_o} = \frac{\alpha\theta Eh\, a^2}{\pi^2 D[(1-\nu) + \frac{ah}{2A_1}]} = \frac{\psi}{[(1-\nu) + \frac{\lambda_1 \pi^2}{8}]} \tag{41}$$

where ψ and λ_1 are defined by equations (37) and (14) respectively. Then the flutter boundary for this case can be plotted by using the top

curves of Figure 6 of reference 1 and replacing the labels R_{x_o} and R_{y_o} in accordance with the above equation. The result is shown in Figure 11(a). The curve is terminated at point T, which corresponds to the point where flutter and static buckling coalesce. Reference 1 did not give the static buckling curve and so it is not given in Figure 11(a). However, the points where the static buckling curve intersects the ψ-axis correspond to static buckling under uniform biaxial compression in the absence of wind, and therefore they were readily obtained from reference 9 and are shown in Figure 11(a) as points P and Q. Figure 11(b) is a replot of Figure 11(a). for the same values of λ_1 and ν that were used in presenting results for cases 1 and 2, namely $\lambda_1 = 1.0$ and $\nu = 0.3$.

Summary of Numerical Results

Figure 12 summarizes (in curves labeled 1, 2, and 3) the numerical flutter results discussed above. Curves (1) and (2) are both for the case of a sinusoidal pillow-shaped temperature distribution but with differing edge-stiffener flexibility: curve (1) corresponds to the perfectly flexible case and curve (2) to the flexurally rigid case. Curve (3) and points P and Q are for the discontinuous temperature distribution with flexurally rigid edge-stiffeners. (Curves (1), (2) and (3) correspond to cases 1, 2, and 3 respectively.) For comparison, the results of Schaeffer and Heard (ref. 1) for an unstiffened plate with a pillow-shaped (parabolic) temperature distribution are presented as curve (0).

Discussion of Numerical Results

From the summary of numerical results (Fig. 12) or from the individual results (Figs. 9, 10, 11 and Fig. 4 of Ref. 6), it is seen that the critical value of λ for flutter decreases as the temperature parameter ψ increases.

This is to be expected because of the compressive stresses induced in the plate by the temperature distribution.

To see in detail the effects of different boundary conditions or different temperature distributions, it is advantageous to study the curves of Figure 12 in adjacent pairs.

First consider curves (0) and (1). These are both for the same pillow-shaped temperature distribution (if we neglect the small difference between the sinusoidal and the parabolic shapes), and differ only by virtue of the fact that curve (0) is for completely unstiffened edges while curve (1) is for edge stiffeners of zero flexural stiffness but of finite axial stiffness. The marked lowering of curve (1) relative to curve (0) is undoubtedly due to the higher compressive stresses arising in the plate due to the additional restraint against thermal expansion provided by the axial stiffness of the edge stiffeners.

Now consider curves (1) and (2). These are for the same pillow-shaped temperature distribution and the same axial stiffness of stiffeners, and differ only in the flexural stiffness of the stiffeners, with curve (2) corresponding to infinite flexural stiffness (stiffeners held straight) and curve (1) corresponding to negligible flexural stiffness. Again, the lowering of curve (2) relative to curve (1) can be ascribed to the higher compressive stresses resulting from the higher constraint against thermal expansion of the plate.

Finally, consider curves (2) and (3). These correspond to the same edge-stiffener conditions (finite axial stiffness, infinite flexural stiffness) and same stiffener temperature of zero, and differ only in respect to the plate temperatures, with curve (2) corresponding to a pillow-shaped temperature distribution of *maximum* value θ , while

curve (3) corresponds to a plate temperature distribution *uniform* at the value θ. In the former case the cooler outer portions of the plate tend to restrain partly the thermal expansion of the inner portion of the plate, whereas in the latter case this restraint is absent. As a result the plate as a whole tends to undergo more thermal expansion and hence develops higher compressive stresses when this thermal expansion is restrained by the stiffeners. Thus the lowering of curve (3) with respect to curve (2) is to be expected.

For $\psi = 0$ there are no thermal stresses in the plate regardless of the presence or absence of edge-stiffeners. Consequently, all four curves of Figure 12 emanate from the same point on the λ axis.

CONCLUDING REMARKS

A theoretical analysis has been made of the supersonic flutter of a rectangular plate with edge stiffeners under non-uniform temperature distribution, producing midplane thermal stresses. Numerical results, obtained for the case of a square plate, show that the presence of the stiffeners has a marked effect on the midplane stresses and therefore on the flutter speed. This effect was found to depend significantly on the axial stiffness of the stiffeners, the flexural stiffness of the stiffeners, and the kind of temperature distribution.

APPENDIX A

LIST OF SYMBOLS

Remarks: i) The subscript 1 or 3 on a symbol for a stiffener-related quantity identifies the stiffener location as $x=o,a$ or $y=o,b$ respectively. ii) The Fourier coefficients of known quantities (loads, thermal strains), and combinations of such coefficients are generally represented by capital letters, while the Fourier coefficients of initially unknown quantities (internal stress,etc.) are denoted by small letters. iii) A parenthetical reference to an equation number in the list below will indicate the equation in which the symbol is first used.

a	plate dimension (see Fig. 1)
a_{pq}	Fourier coefficients in series expansion for lateral deflection $w(x,y,t)$, (eq. 32).
$\bar{a}_{pq}(t)$	Fourier coefficient in series expansion for lateral deflection $w(x,y,t)$, (eq. B-1).
A_1, A_3	Stiffener cross-sectional areas
A_{mn}	See equation (10)
b	Plate dimension (see Fig. 1)
B_n' and B_m'''	Fourier coefficients in series expansion for $N_1(y)$ and $N_3(x)$ respectively, (eq. 7)
B_n	$B_n'/\alpha\theta Eh$
c_{mn}	Fourier coefficients in series expansion for $N_y(x,y)$, (eq. 8)
c_n'	Fourier coefficient in series expansions for $N_y(o,y)$, (eq. 8)
C_n	$c_n'/\alpha\theta Eh$

$\bar{c}_n'$	$c_n' \left(\frac{1}{Eh}\right) \left(\frac{n\pi}{b}\right)$
C_{mn}	See equation (36)
D	$Eh^3/[12(1-\nu^2)]$
$e_1(y)$ and $e_3(x)$	Stiffener thermal strains
$e_x(x,y)$ and $e_y(x,y)$	Plate thermal strains
$\bar{E}_{mn}$	See equation (21)
E_{mn}	See equation (9a)
g_{mn}	Fourier coefficients in series expansion for $N_x(x,y)$, (eq. 8)
g_m'	Fourier coefficients in series expansion for $N_x(x,o)$, (eq. 8)
G_{mn}	See equation (36)
h	Thickness of plate
H_{mn}	See equation (21)
j_{mn}	Fourier coefficients in series expansion for $N_{xy}(x,y)$, (eq. 8)
K^2	Frequency parameter, $\mu h a^4 \omega^2/D\pi^4$
K_{mn}	See equation (9a)
K_n', K_m'''	Fourier coefficients in series expansion for prescribed boundary curvatures, (eq. 17)
ℓ	Aerodynamic forces, $-[2q^*/\sqrt{M^2-1}]\,\partial\omega/\partial x$
m,n,p,q,r,s	Summation indexes
M	Upper limit of Fourier series
M	Mach number
n	Summation index
N	Upper limit of Fourier series

$N_1(y)$, $N_3(x)$	External running tensions, force per unit length
N_x, N_y, N_{xy}	Plate stress resultants, for per unit length
p	Summation index
$p_1(y)$, $p_3(x)$	Stiffener cross-sectional tensions
P,Q	Integers appearing in sinusoidal temperature distribution, (eq. 1)
q*	$(1/2)\rho V^2$
q	Summation index
r	Summation index
R	Upper limit of Fourier series
R_n' R_m'''	See equation (9a)
R_{x_o}	External load parameter (ref. 1),- N_x $a^2/\pi^2 D$
R_{y_o}	External load parameter (ref. 1),- N_y $a^2/\pi^2 D$
s	Summation index
S	Upper limit of Fourier series
s_n', s_m'''	Fourier coefficient in series expansion for the stiffener cross-sectional tensions
S_n', S_m'''	See equation (21)
T(x,y)	Temperature distribution (eq. 1)
T_1, T_3	External resultant loading
T_{mn}	Fourier coefficient see equation (5)
T_n', T_m'''	Fourier coefficients in series expansion for thermal strain discontinuities between stiffener and plate edge, (eq. 5)
t	Time

u,v	x and y components of displacements in plate
V	Velocity of air stream
V_n', V_m'''	Fourier coefficients in series expansion for $\partial e_y/\partial x$ etc. (eq. 16)
$w(x,y,t)$	Lateral plate deflection
x,y	Cartesian co-ordinates
α	Coefficient of thermal expansion of plate and stiffeners
$[\alpha_1(n) - \beta_1(n)]$	See equation (21)
$[\alpha_3(m) - \beta_2(m)]$	See equation (21)
$[\gamma_n' - \gamma_n'']$	See equation (21)
$[\gamma_n^{(1)} - \gamma_n^{(2)}]$	See equation (21)
$[\Gamma_m' - \Gamma_m'']$	See equation (21)
$[\Gamma_m^{(1)} - \Gamma_m^{(2)}]$	See equation (21)
δ_{ij}	Kronecker's delta
δ_n',δ_m'''	See equation (21)
Δ	Determinant of the coefficient of a_{rs}
Δ'	Determinant of the coefficients of those a_{rs} with second subscript odd.
Δ''	Determinant of the coefficients of those a_{rs} with second subscripts even
θ	Temperature rise at the center of plate
λ_1	Area-ratio parameter, $4ah/\pi^2 A_1$ (eq. 14)
λ	Aerodynamic pressure parameter, $2q^* a^3/D\sqrt{M^2-1}$ (eq. 33)

λ_{cr}	Critical flutter speed
Λ_{mn}' Λ_{mn}''	See equation (21)
μ	Mass density of plate
μ_{mn}', μ_{mn}''	See equation (21)
ν	Poissons ratio
ν_{mn}', ν_{mn}''	See equation (21)
π_{mn}	See equation (21)
ρ	Mass density of air
ψ	$\alpha\theta Eh/D\pi^2$, (eq. 37)
ω	Circular frequency, radians per unit time

APPENDIX B

The purpose of this appendix is to justify heuristically the assumption made in the body of the paper to the effect that the general motion of the plate can be represented as a sum of terms, each of the type shown on the right side of equation (32).

To that end we start by assuming a more general form for the motion, namely

$$w(x,y,t) = \sum_{p=1}^{R} \sum_{q=1}^{S} \bar{a}_{pq}(t) \sin \frac{p\pi x}{a} \sin \frac{q\pi y}{b} \qquad \text{(B-1)}$$

in which the $\bar{a}_{pq}$ (in contrast to the a_{pq}'s of eq. 32) are undetermined functions of time. From the theory of Fourier series, it is known that equation B-1 with sufficiently large R and S is capable of representing the lateral motion of a simply supported rectangular plate to any desired degree of accuracy.

Substituting equation B-1 into the basic differential equation (2) for the motion of the plate, replacing N_x, N_y, N_{xy} by their Fourier series (eq. 10) and ℓ by its expression $- 2q^* (\partial w/\partial x)/\sqrt{M^2-1}$ gives:

$$\sum_{p=1}^{R} \sum_{q=1}^{S} \bar{a}_{pq}(t) \sin \frac{p\pi x}{a} \sin \frac{q\pi y}{b} \left[\left(\frac{p\pi}{a}\right)^2 + \left(\frac{q\pi}{b}\right)^2\right]^2$$

$$+ \frac{1}{D} \sum_{m,n\ \text{odd}}^{M,N} \sum_{p=1}^{R} \sum_{q=1}^{S} \bar{a}_{pq}(t) \sin \frac{m\pi x}{a} \sin \frac{n\pi y}{b} \sin \frac{p\pi x}{a} \sin \frac{q\pi y}{b} \left[\left(\frac{p\pi}{a}\right)^2 g_{mn} + \left(\frac{q\pi}{b}\right)^2 c_{mn}\right]$$

$$+ \frac{2}{D} \sum_{m,n\ \text{odd}}^{M,N} \sum_{p=1}^{R} \sum_{q=1}^{S} \bar{a}_{pq}(t) \cos \frac{p\pi x}{a} \cos \frac{q\pi y}{b} \cos \frac{m\pi x}{a} \cos \frac{n\pi y}{b} \left[\left(\frac{p\pi}{a}\right)\left(\frac{q\pi}{b}\right) j_{mn}\right]$$

$$+ \sum_{p=1}^{R} \sum_{q=1}^{S} \bar{a}_{pq}(t) \frac{2q^*}{D\sqrt{M^2-1}} \left(\frac{p\pi}{a}\right) \sin \frac{q\pi y}{b} \cos \frac{p\pi x}{a} + \frac{\mu h}{D} \sum_{p=1}^{R} \sum_{q=1}^{S} \ddot{\bar{a}}_{pq}(t) \sin \frac{p\pi x}{a} \sin \frac{q\pi y}{b} = 0 \qquad \text{(B-2)}$$

where $\ddot{\bar{a}}_{pq}(t)$ stands for the second derivative of $\bar{a}_{pq}(t)$ with respect to time. Multiplying this equation by $\sin(r\pi x)/a \sin(s\pi y)/b$, where r and s are any integers, and integrating over the whole region of the plate, one obtains the following system of ordinary differential equations for the functions $\bar{a}_{pq}(t)$:

$$\bar{a}_{rs}(t)\left[\left(\frac{r}{a}\right)^2+\left(\frac{s}{b}\right)^2\right]^2+\sum_{m,n\ \text{odd}}^{M,N}\sum_{\substack{p=1\\ q+s=\text{even}}}^{R,S} 16\,\bar{a}_{pq}(t)\,\frac{pqrs}{D\pi^4}\left\{\frac{4mn\left[\left(\frac{p}{a}\right)^2 g_{mn}+\left(\frac{q}{b}\right)^2 c_{mn}\right]+\frac{\epsilon}{ab}\,j_{mn}\,(r^2-m^2-p^2)(s^2-n^2-q^2)}{[(m-p+r)(m-p-r)(m+p+r)(m+p-r)][(n-q+s)(n-q-s)(n+q+s)(n+q-s)]}\right\}$$

$$+\frac{\mu h}{D\pi^4}\ddot{\bar{a}}_{rs}(t)+\frac{2\lambda}{a^4\pi^4}\sum_{\substack{p=1\\ p\neq r}}^{R} rp\,\bar{a}_{ps}(t)\,\frac{[1-(-1)^{p+r}]}{[r^2-p^2]}=0 \qquad \text{(B-3)}$$

$$\text{for}\quad r=1,2,\ldots,R$$
$$s=1,2,\ldots,S$$

The above equations are linear and homogeneous differential equations with constant coefficients. Such a system is known to have, in general, a solution of the following form:

$$\bar{a}_{pq}(t)=\sum_{m} a_{pq}^{(m)}\, e^{i\omega_m t} \qquad \text{(B-4)}$$

where the ω_m are the roots of a characteristic equation obtained by equating to zero the determinant of the coefficients of a certain system of homogeneous algebraic equations. For any given value of m, the relative

magnitudes of the $a_{pq}^{(m)}$ are determined by substituting the particular value of ω_m into this system of algebraic equations.

In view of equation B-4, the general motion, equation B-1, has the form

$$w(x,y,t) = \sum_{m} \left\{ \sum_{p=1}^{R} \sum_{q=1}^{S} a_{pq}^{(m)} \sin \frac{p\pi x}{a} \sin \frac{q\pi y}{b} \right\} e^{i \omega_m t} \tag{B-5}$$

The right hand side of this equation is a sum of terms, each of the form of the right hand side of equation (32).

TABLE 1

Results of Solving Simultaneous Equations 13 and 24

for the Case $M = 59$, $\lambda_1 = 1$, $P = Q = 1$

	(a)	(b)	(c)
	Case 1	Case 2	
n	C_n	C_n	B_n
1	0.2014886	0.2604108	-0.3068841
3	-0.005111925	0.09404856	0.0520033
5	-0.00130178	0.06144001	0.03772039
7	-0.000493739	0.04557436	0.03010360
9	-0.0002351824	0.03622673	0.02508517
11	-0.0001292827	0.03006727	0.02150895
13	-0.0000783595	0.02570173	0.01882797
15	-0.0000509683	0.02244517	0.01674201
17	-0.0000349673	0.01992211	0.01507195
19	-0.0000250098	0.01790943	0.01370412
21	-0.0000184955	0.01626622	0.01256302
23	-0.0000140577	0.01489917	0.01159634
25	-0.00001093168	0.01374395	0.01076678
27	-0.00000866683	0.01275479	0.01004704
29	-0.000006986196	0.01189826	0.009416610
31	-0.00000571312	0.01114930	0.008859836
33	-0.0000047312	0.01048888	0.008364495
35	-0.00000396182	0.009902135	0.007920992
37	-0.00000335048	0.009377394	0.007521577
39	-0.00000285864	0.008905318	0.007160012
41	-0.00000245848	0.008478362	0.006831195
43	-0.000002129615	0.008090362	0.006530862
45	-0.00000185685	0.007736210	0.006255489
47	-0.0000016287	0.00741674	0.006002109
49	-0.00000143647	0.007113181	0.005768187
51	-0.00000127331	0.006837726	0.005551599
53	-0.000001133943	0.006582752	0.00535050
55	-0.000001014188	0.006346043	0.005163275
57	-0.0000009107152	0.006125722	0.004988555
59	-0.0000008208478	0.005920138	0.004825130

TABLE 2.

System of Equations for the Unknown Amplitude Coefficients, a_{pq}, Obtained for Dynamic Behavior of Square Plate for Case 1: Pillow-Shaped Temperature Distribution, Stiffeners Perfectly Flexible, $\nu_1 = 1$, P = Q = 1, M = N = 59, R = 6 and S = 5.

$4-K^2$ -0.415214ψ	0.338875ψ	0.104855ψ	-0.02737λ	-0.01095λ	-0.00704λ	0.338875ψ	0.231425ψ	0.107328ψ	0.104861ψ	0.107358ψ	0.046683ψ	0.0	0.0	0.0	0.0	0.0	0.0	a_{11}
0.338893ψ	$100\ -K^2$ -2.00468ψ	1.235197ψ	0.04927λ	-0.07039λ	-0.02737λ	-0.55649ψ	0.731445ψ	0.479669ψ	-0.191049ψ	0.155359ψ	0.255681ψ	0.0	0.0	0.0	0.0	0.0	0.0	a_{31}
0.104861ψ	1.235181ψ	$676\ -K^2$ -5.321112ψ	0.01955λ	0.09124λ	-0.1198λ	-0.191063ψ	-1.358461ψ	1.699617ψ	-0.065398ψ	-0.439758ψ	0.319419ψ	0.0	0.0	0.0	0.0	0.0	0.0	a_{51}
0.02737λ	-0.04927λ	-0.01955λ	$25\ -K^2$ -0.977079ψ	0.720309ψ	0.208079ψ	0.0	0.0	0.0	0.0	0.0	0.0	0.440504ψ	0.380569ψ	0.186099ψ	0.108042ψ	0.186855ψ	0.082625ψ	a_{21}
0.01095λ	0.07039λ	-0.09124λ	0.720309ψ	$289\ -K^2$ -3.454304ψ	1.892226ψ	0.0	0.0	0.0	0.0	0.0	0.0	-0.950523ψ	1.153253ψ	0.533053ψ	-0.316858ψ	0.226551ψ	0.315873ψ	a_{41}
0.00704λ	0.02737λ	0.11198λ	0.208094ψ	1.892245ψ	$1369\ -K^2$ -7.603892ψ	0.0	0.0	0.0	0.0	0.0	0.0	-0.338641ψ	-1.79976ψ	2.36891ψ	-0.114429ψ	-0.566691ψ	0.433407ψ	a_{61}
0.338893ψ	-0.55631ψ	-0.191051ψ	0.0	0.0	0.0	$100-K^2$ -2.004677ψ	0.731462ψ	0.155360ψ	1.235194ψ	0.479669ψ	0.255653ψ	-0.02737λ	-0.01095λ	-0.00704λ	0.0	0.0	0.0	a_{13}
0.231416ψ	0.731462ψ	-1.35848ψ	0.0	0.0	0.0	0.731445ψ	$324\ -K^2$ -2.452424ψ	1.43776ψ	-1.35829ψ	1.43776ψ	1.30851ψ	0.04927λ	-0.07039λ	-0.02737λ	0.0	0.0	0.0	a_{33}
0.107374ψ	0.479643ψ	1.699601ψ	0.0	0.0	0.0	0.155385ψ	1.43759ψ	$1156\ -K^2$ -4.58477ψ	-0.439758ψ	-2.978872ψ	2.607603ψ	0.01955λ	0.09124λ	-0.11198λ	0.0	0.0	0.0	a_{53}
0.104829ψ	-0.191063ψ	-0.065415ψ	0.0	0.0	0.0	1.23501ψ	-1.35848ψ	-0.439732ψ	$676\ -K^2$ -5.321112ψ	1.699601ψ	0.319438ψ	0.0	0.0	0.0	-0.02737λ	-0.01095λ	-0.00704λ	a_{15}
0.107374ψ	0.155368ψ	-0.439751ψ	0.0	0.0	0.0	0.479641ψ	1.43761ψ	-2.978896ψ	1.699617ψ	$1156\ -K^2$ -4.584768ψ	2.607631ψ	0.0	0.0	0.0	0.04927λ	-0.07039λ	-0.02737λ	a_{35}
0.046681ψ	0.255667ψ	0.319437ψ	0.0	0.0	0.0	0.255667ψ	1.30872ψ	2.607621ψ	0.319419ψ	2.607603ψ	$2500\ -K^2$ -6.65772ψ	0.0	0.0	0.0	0.01955λ	0.09124λ	-0.11198λ	a_{55}
0.0	0.0	0.0	0.440521ψ	-0.950509ψ	-0.338619ψ	0.02737λ	-0.04927λ	-0.01955λ	0.0	0.0	0.0	$169\ -K^2$ -1.864775ψ	1.068989ψ	0.253011ψ	1.12066ψ	0.921753ψ	0.462779ψ	a_{23}
0.0	0.0	0.0	0.380592ψ	1.153279ψ	-1.79993ψ	0.01095λ	0.07039λ	-0.09124λ	0.0	0.0	0.0	1.068979ψ	$625\ -K^2$ -3.373579ψ	1.883787ψ	-2.18311ψ	1.94229ψ	1.64048ψ	a_{43}
0.0	0.0	0.0	0.186073ψ	0.533075ψ	2.36879ψ	0.00704λ	0.02737λ	0.11198λ	0.0	0.0	0.0	0.253023ψ	1.883761ψ	$2025\ -K^2$ -6.07532ψ	-0.7599ψ	-3.801341ψ	3.42717ψ	a_{63}
0.0	0.0	0.0	0.108051ψ	-0.316871ψ	-0.114457ψ	0.0	0.0	0.0	0.02737λ	-0.04927λ	-0.01955λ	1.120671ψ	-2.18321ψ	-0.759812ψ	$841\ -K^2$ -4.18997ψ	2.19402ψ	0.472589ψ	a_{25}
0.0	0.0	0.0	0.1868724ψ	0.226572ψ	-0.566681ψ	0.0	0.0	0.0	0.01095λ	0.07039λ	-0.09124λ	0.92176ψ	1.94215ψ	-3.80135ψ	2.19402ψ	$1681\ -K^2$ -5.41096ψ	3.06358ψ	a_{45}
0.0	0.0	0.0	0.082609ψ	0.315851ψ	0.433429ψ	0.0	0.0	0.0	0.00704λ	0.02737λ	0.11198λ	0.462761ψ	1.64047ψ	3.42701ψ	0.472561ψ	3.063561ψ	$3721\ -K^2$ -7.965497ψ	a_{65}

$= [0]$

TABLE 3.

System of Equations for the Unknown Amplitude Coefficients, a_{pq}, Obtained for Dynamic Behavior of Square Plate for Case 2: Pillow-Shaped Temperature Distribution, Stiffeners Flexurally Rigid, $\lambda_1 = 1$, P = Q = 1, M = N = 59, R = 6 and S = 5.

$4-K^2$ -0.703221ψ	0.224017ψ	0.048415ψ	-0.02737λ	-0.01095λ	-0.00704λ	0.224032ψ	0.08151ψ	0.033211ψ	0.048498ψ	0.033211ψ	0.007281ψ	0.0	0.0	0.0	0.0	0.0	0.0	a_{11}
0.224032ψ	$100-K^2$ -3.386544ψ	0.593106ψ	0.04927λ	-0.07039λ	-0.02737λ	-0.240493ψ	1.092897ψ	0.161032ψ	-0.076366ψ	0.153868ψ	0.094981ψ	0.0	0.0	0.0	0.0	0.0	0.0	a_{31}
0.048498ψ	0.593282ψ	$676-K^2$ -9.0051ψ	0.01955λ	0.09124λ	-0.11198λ	-0.076344ψ	-0.580676ψ	2.91237ψ	-0.010065ψ	-0.139421ψ	0.411027ψ	0.0	0.0	0.0	0.0	0.0	0.0	a_{51}
0.02737λ	-0.04927λ	-0.01955λ	$25-K^2$ -1.64438ψ	0.386032ψ	0.088419ψ	0.0	0.0	0.0	0.0	0.0	0.0	0.52503ψ	0.13351ψ	0.05445ψ	0.07484ψ	0.06386ψ	0.01349ψ	a_{21}
0.01095λ	0.07039λ	-0.09124λ	0.386109ψ	$289-K^2$ -5.8426ψ	0.854127ψ	0.0	0.0	0.0	0.0	0.0	0.0	-0.40364ψ	1.889127ψ	0.16523ψ	-0.10917ψ	0.26655ψ	0.12574ψ	a_{41}
0.00704λ	0.02737λ	0.11198λ	0.088692ψ	0.854451ψ	$1369-K^2$ -12.8719ψ	0.0	0.0	0.0	0.0	0.0	0.0	-0.1429ψ	-0.77706ψ	4.1627ψ	-0.017056ψ	-0.169898ψ	0.58697ψ	a_{61}
0.224032ψ	-0.240493ψ	-0.076344ψ	0.0	0.0	0.0	$100-K^2$ -3.38654ψ	1.092887ψ	0.15382ψ	0.59313ψ	0.161089ψ	0.095028ψ	-0.02737λ	-0.01095λ	-0.00704λ	0.0	0.0	0.0	a_{13}
0.081053ψ	1.092897ψ	-0.580676ψ	0.0	0.0	0.0	1.092899ψ	$324-K^2$ -3.99691ψ	1.49995ψ	-0.58073ψ	1.49995ψ	0.511061ψ	0.04927λ	-0.07039λ	-0.02737λ	0.0	0.0	0.0	a_{33}
0.03329ψ	0.161032ψ	2.91237ψ	0.0	0.0	0.0	0.153869ψ	1.49995ψ	$1156-K^2$ -7.48081ψ	-0.139421ψ	-1.18273ψ	3.66415ψ	0.01955λ	0.09124λ	-0.11198λ	0.0	0.0	0.0	a_{53}
0.048498ψ	-0.076366ψ	-0.010065ψ	0.0	0.0	0.0	0.59329ψ	-0.58073ψ	-0.139421ψ	$676-K^2$ -9.005ψ	2.91236ψ	0.410981ψ	0.0	0.0	0.0	-0.02737λ	-0.01095λ	-0.00704λ	a_{15}
0.0332093ψ	0.153869ψ	-0.139423ψ	0.0	0.0	0.0	0.16103ψ	1.49995ψ	-1.18273ψ	2.91237ψ	$1156-K^2$ -7.48081ψ	3.66415ψ	0.0	0.0	0.0	0.04927λ	-0.07039λ	-0.02737λ	a_{35}
0.007282ψ	0.094981ψ	0.411027ψ	0.0	0.0	0.0	0.094981ψ	0.510884ψ	3.66427ψ	0.411028ψ	3.66427ψ	$2500-K^2$ -10.7188ψ	0.0	0.0	0.0	0.01955λ	0.09124λ	-0.11198λ	a_{55}
0.0	0.0	0.0	0.525046ψ	-0.403624ψ	-0.142837ψ	0.02737λ	-0.04927λ	-0.01955λ	0.0	0.0	0.0	$169-K^2$ $-3,030037\psi$	1.326813ψ	0.211054ψ	0.827051ψ	0.349642ψ	0.167979ψ	a_{23}
0.0	0.0	0.0	0.133484ψ	1.88915ψ	-0.776965ψ	0.01095λ	0.07039λ	-0.09124λ	0.0	0.0	0.0	1.32686ψ	$625-K^2$ -5.50376ψ	1.6825ψ	-0.88027ψ	2.44771ψ	0.646118ψ	a_{43}
0.0	0.0	0.0	0.054376ψ	0.165122ψ	4.1627ψ	0.00704λ	0.02737λ	0.11198λ	0.0	0.0	0.0	0.211221ψ	1.68276ψ	$2025-K^2$ $-9,91207\psi$	-0.2526996ψ	-1.50304ψ	5.149327ψ	a_{63}
0.0	0.0	0.0	0.074892ψ	-0.1092ψ	-0.01705ψ	0.0	0.0	0.0	0.02737λ	-0.04927λ	-0.01955λ	0.827171ψ	-0.880292ψ	-0.25262ψ	$841-K^2$ $-6,80734\psi$	3.403574ψ	0.554821ψ	a_{25}
0.0	0.0	0.0	0.063826ψ	0.2666ψ	-0.1699ψ	0.0	0.0	0.0	0.01095λ	0.07039λ	-0.09124λ	0.349555ψ	2.44785ψ	-1.50297ψ	3.40363ψ	$1681-K^2$ $-8,8493\psi$	3.88895ψ	a_{45}
0.0	0.0	0.0	0.01347ψ	0.125689ψ	0.587ψ	0.0	0.0	0.0	0.00704λ	0.02737λ	0.11198λ	0.167863ψ	0.64593ψ	5.14945ψ	0.554981ψ	3.889196ψ	$3721-K^2$ -13.0449ψ	a_{65}

$= [0]$

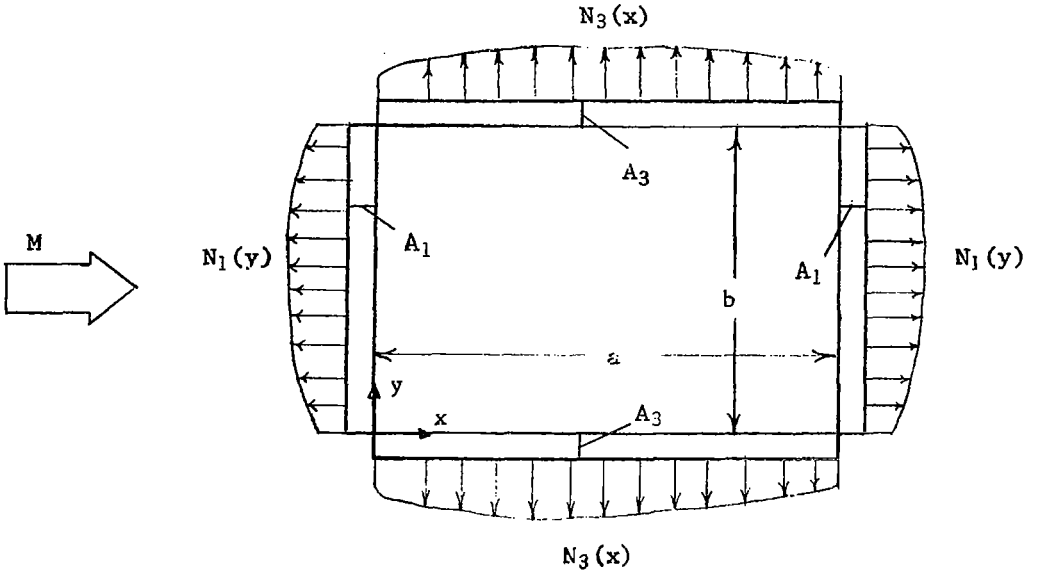

Figure 1. Structure and Loading Considered (Symmetric About Each Centerline).

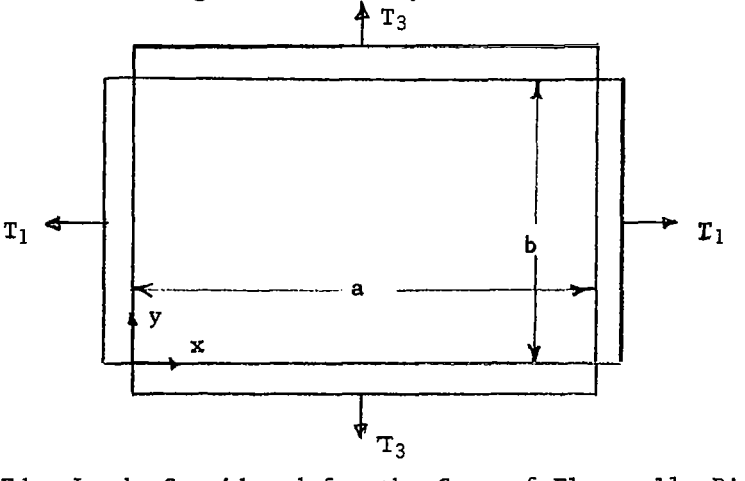

Figure 2. Resultant Edge Loads Considered for the Case of Flexurally Rigid Stiffeners.

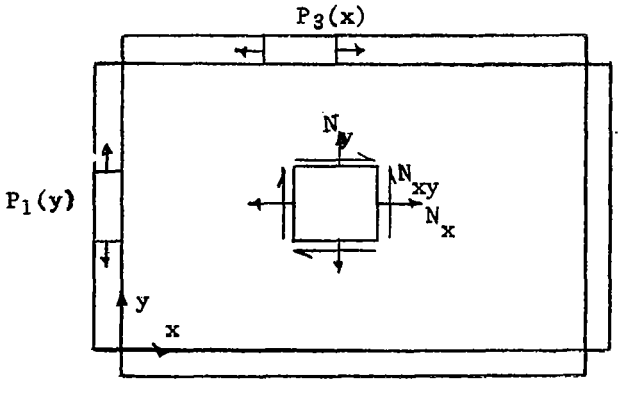

Figure 3. Notation for Stiffener and Plate Forces.

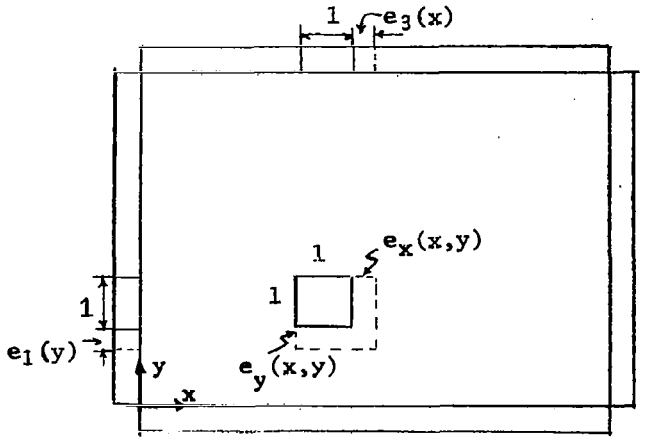

Figure 4. Notation for Thermal Strains.

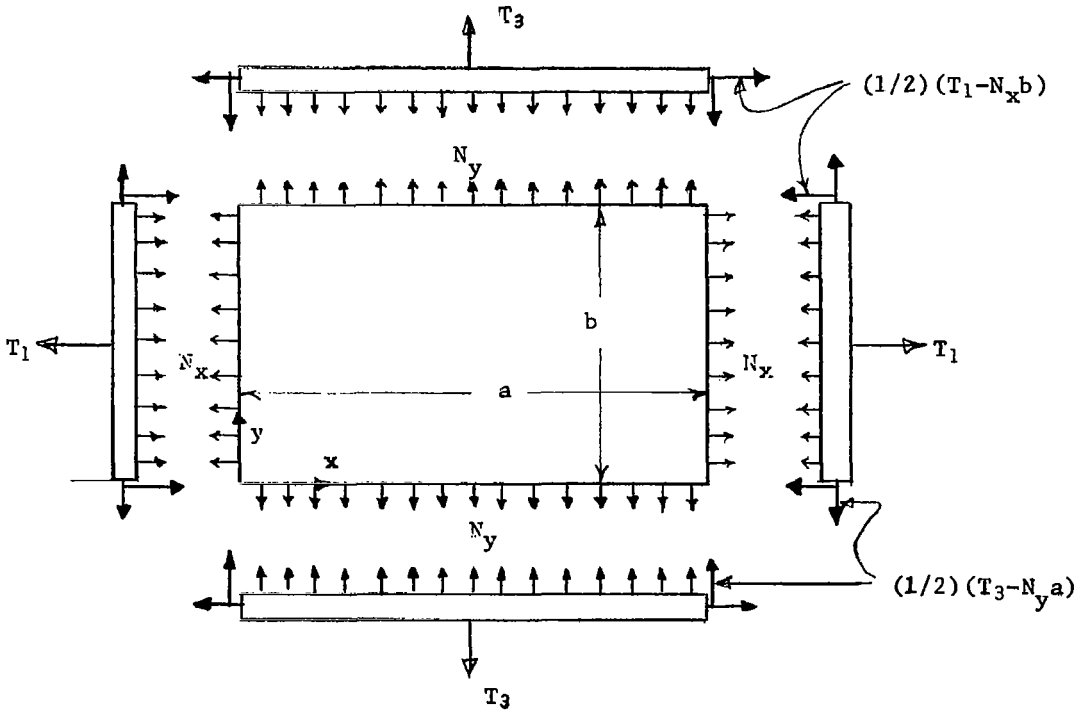

Figure 5. Free-body Diagrams for Case 3: Discontinuous Temperature with Flexurally Rigid Stiffeners.

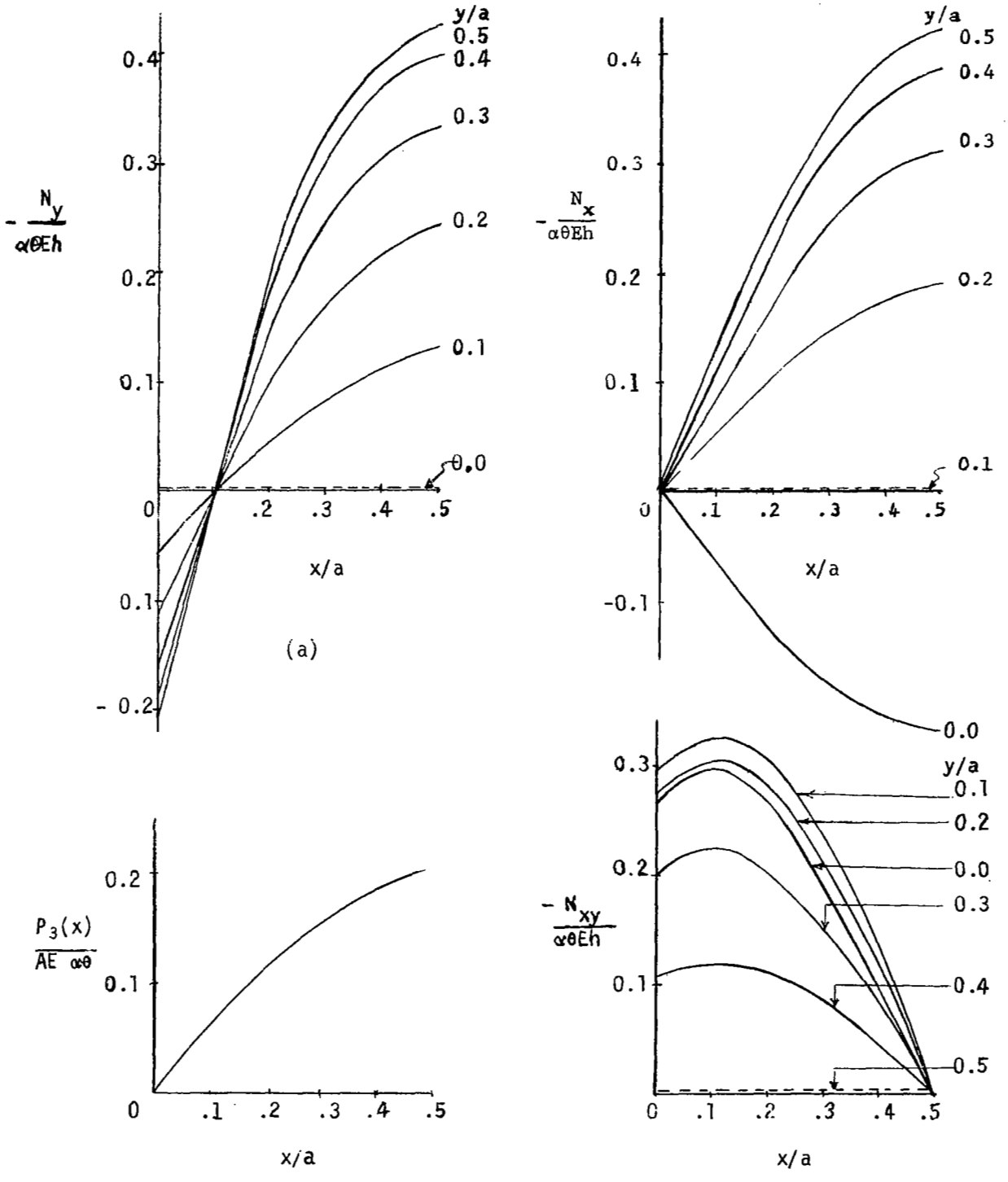

Figure 6. Plate Stresses and Stiffener Tensions for Case 1: Pillow-Shaped (sinusoidal) Temperature Distribution, With Perfectly Flexible Stiffeners. $\lambda_1 = 1, \nu = 0.3$, M = N = 59.

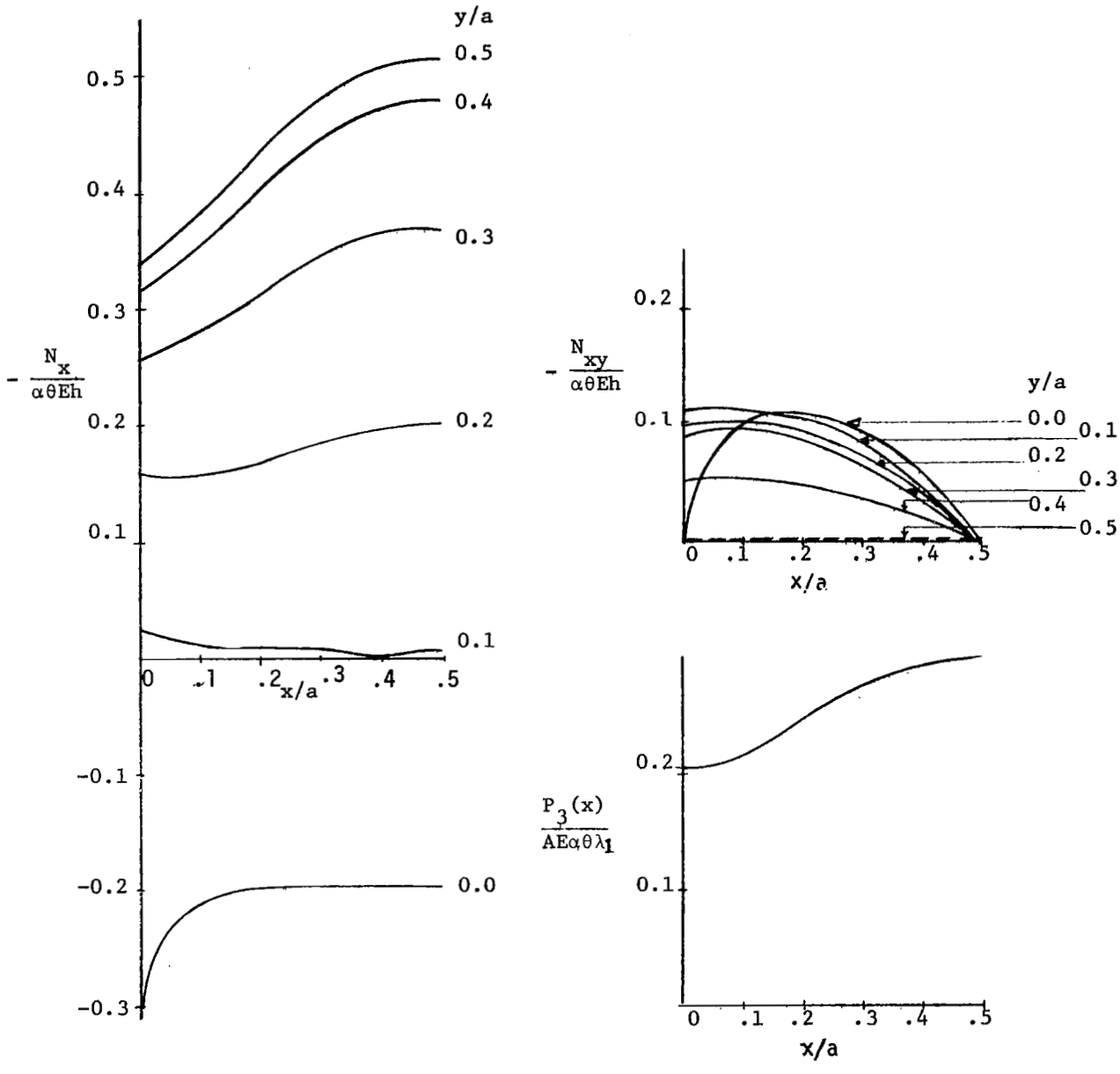

Figure 7. Plate Stresses and Stiffener Tensions for Case 2: Flexurally Rigid Stiffeners, Pillow-Shaped (sinusoidal) Temperature Distribution. $\lambda_1 = 1$, $\nu = 0.3$, M = N = 59.

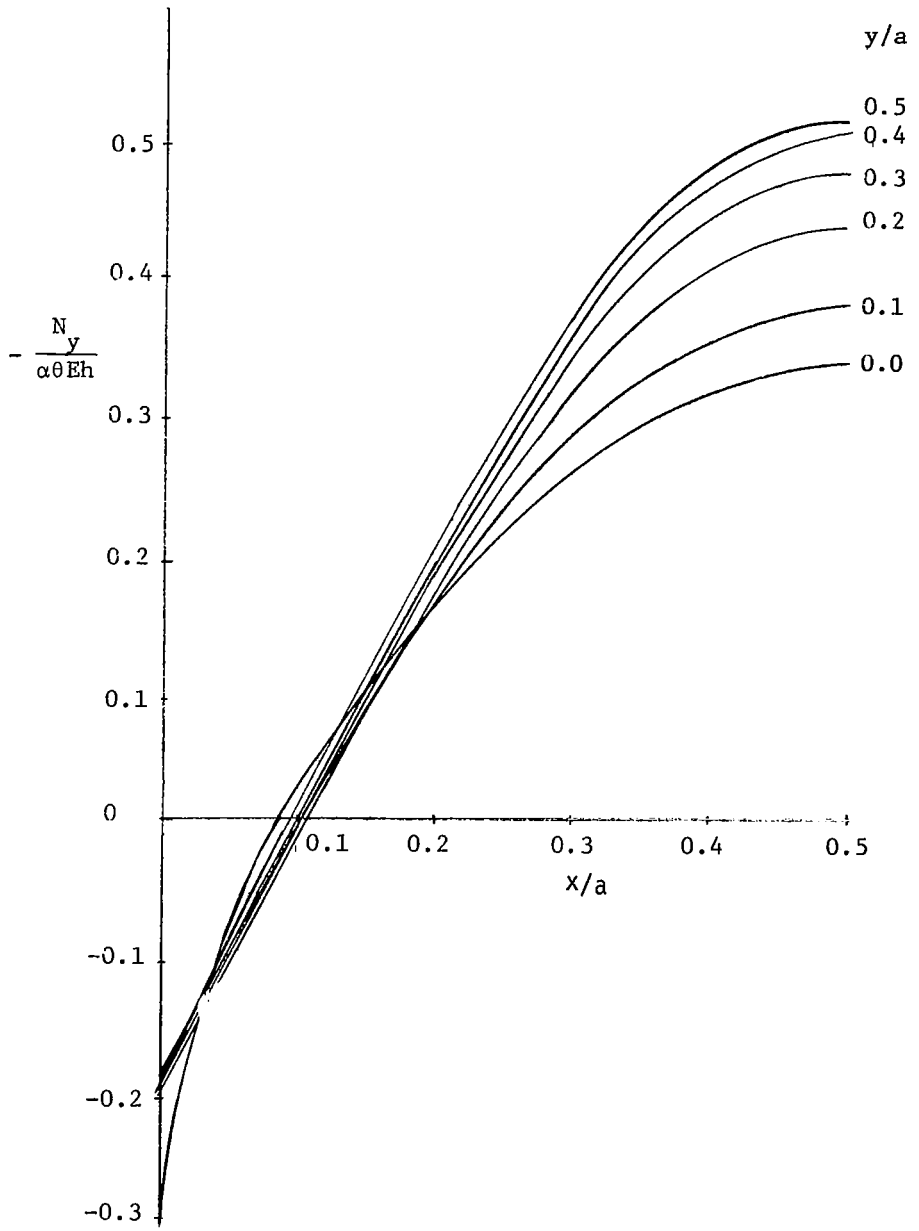

Figure 7. Concluded.

$\psi = 12$

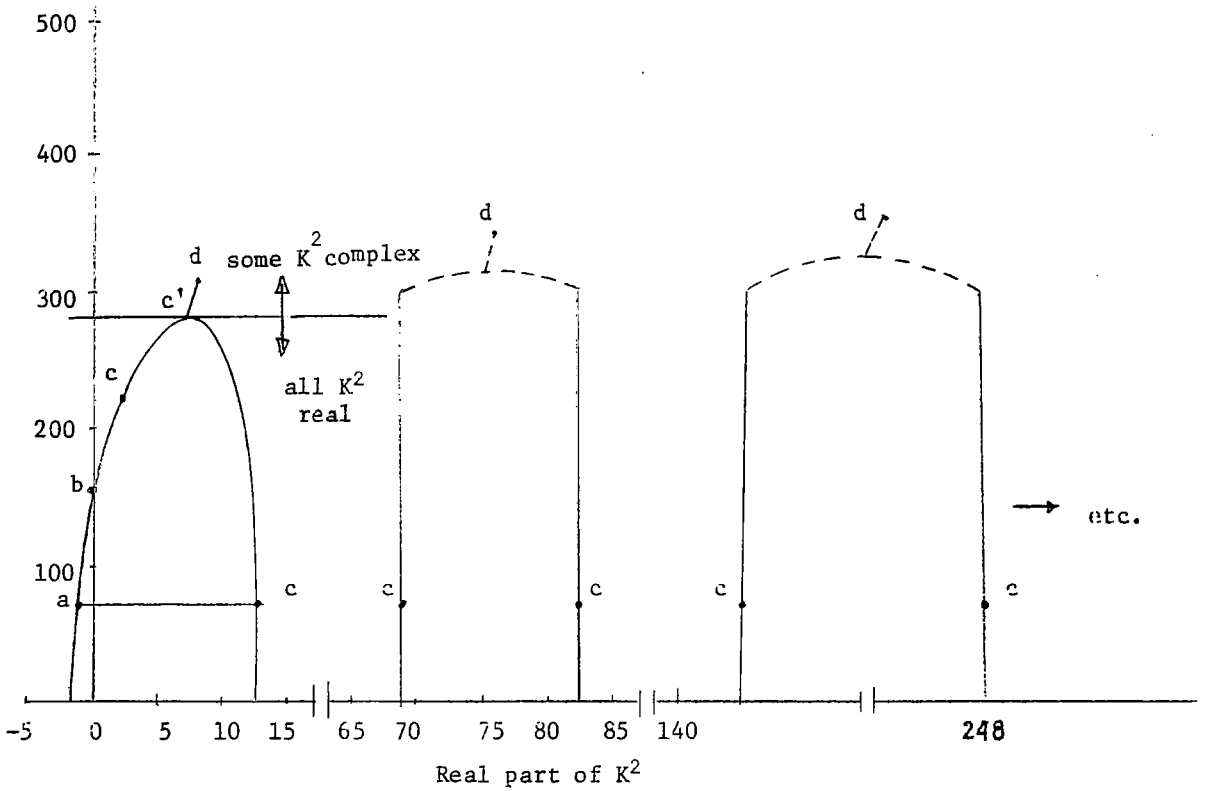

Figure 8. Typical Graph Showing Real Parts of the Roots K^2 as a function of λ for a Fixed Value of ψ (=12) and Given Edge Conditions (Stiffeners Perfectly Flexible, No External Load).

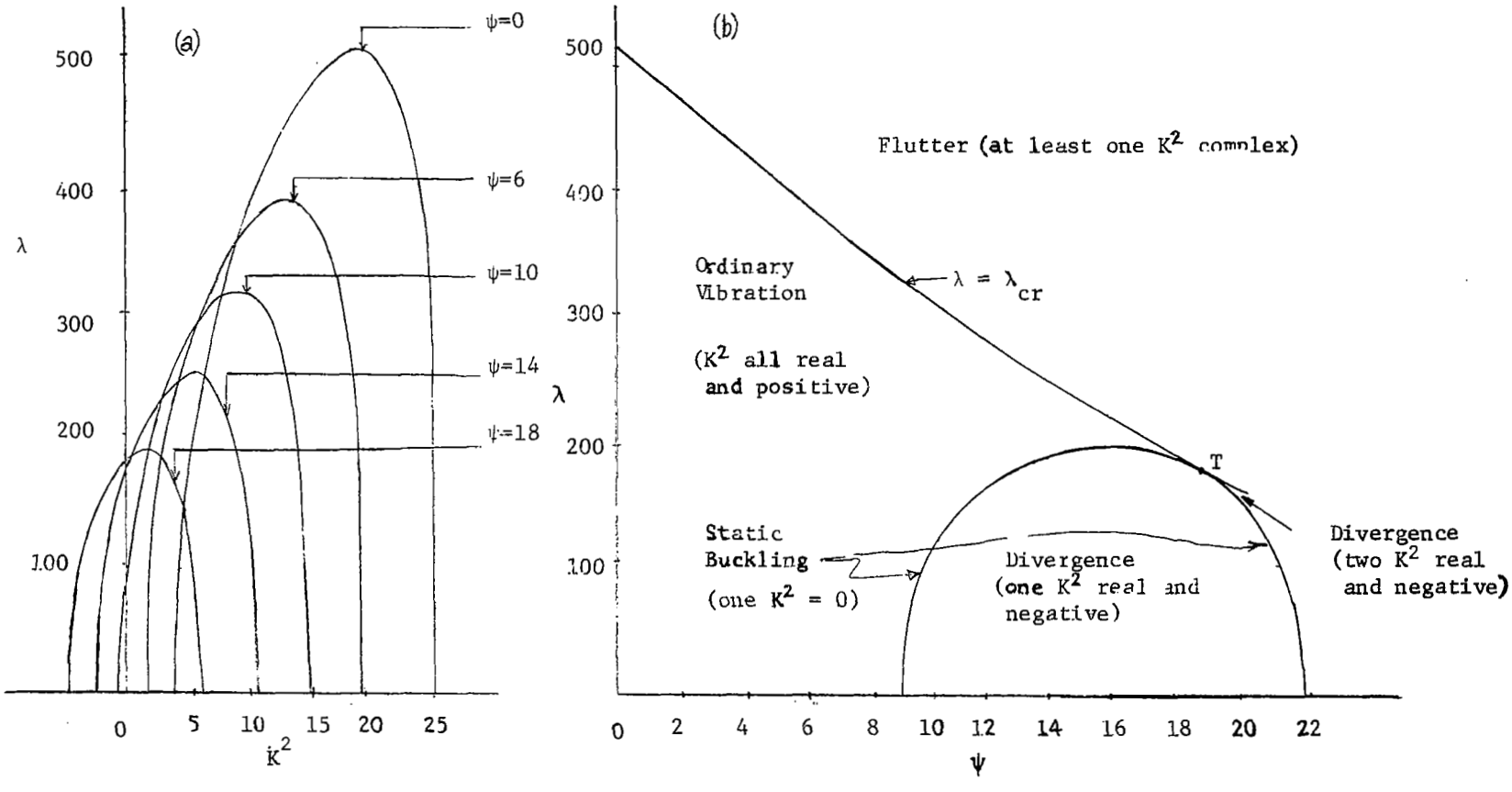

Figure 9.a)Frequency Curves and b) Behavior Regimes for Square Plate with no Externally Applied Load, for Case 1: Perfectly Flexible Stiffeners, Pillow-shaped Temperature Distribution. R = 6, S = 5, M = N = 59, $\lambda_1 = 1$, $\nu = 0.3$.

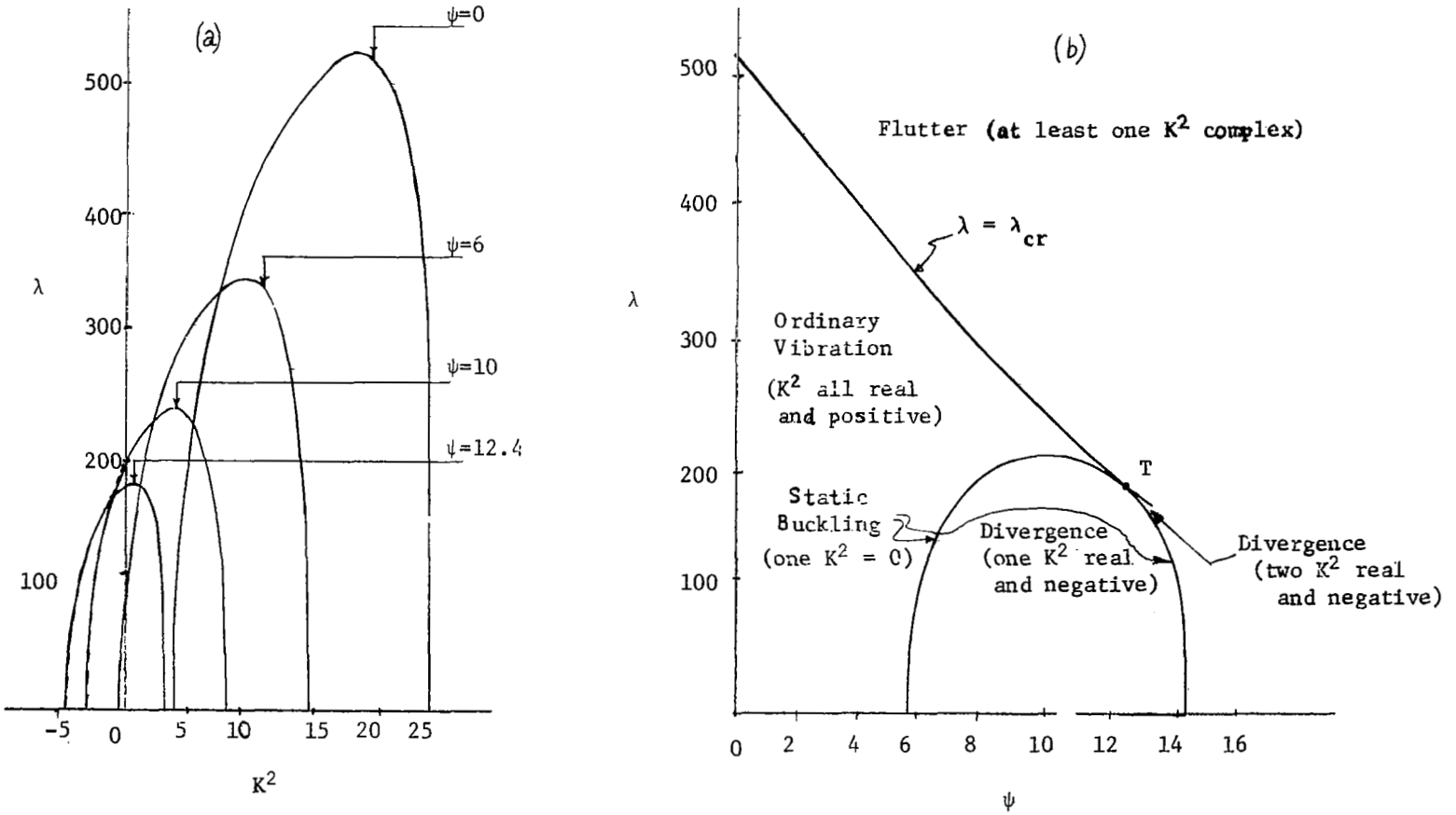

Figure 10. a) Frequency Curves and (b) Behavior Regimes for Square Plate with no Externally Applied Loads for the Case 2: Flexurally Rigid Stiffeners, Pillow-Shaped Temperature Distribution. R = 6, S = 5, M = N = 59, $\lambda_1 = 1$, $\nu = 0.3$.

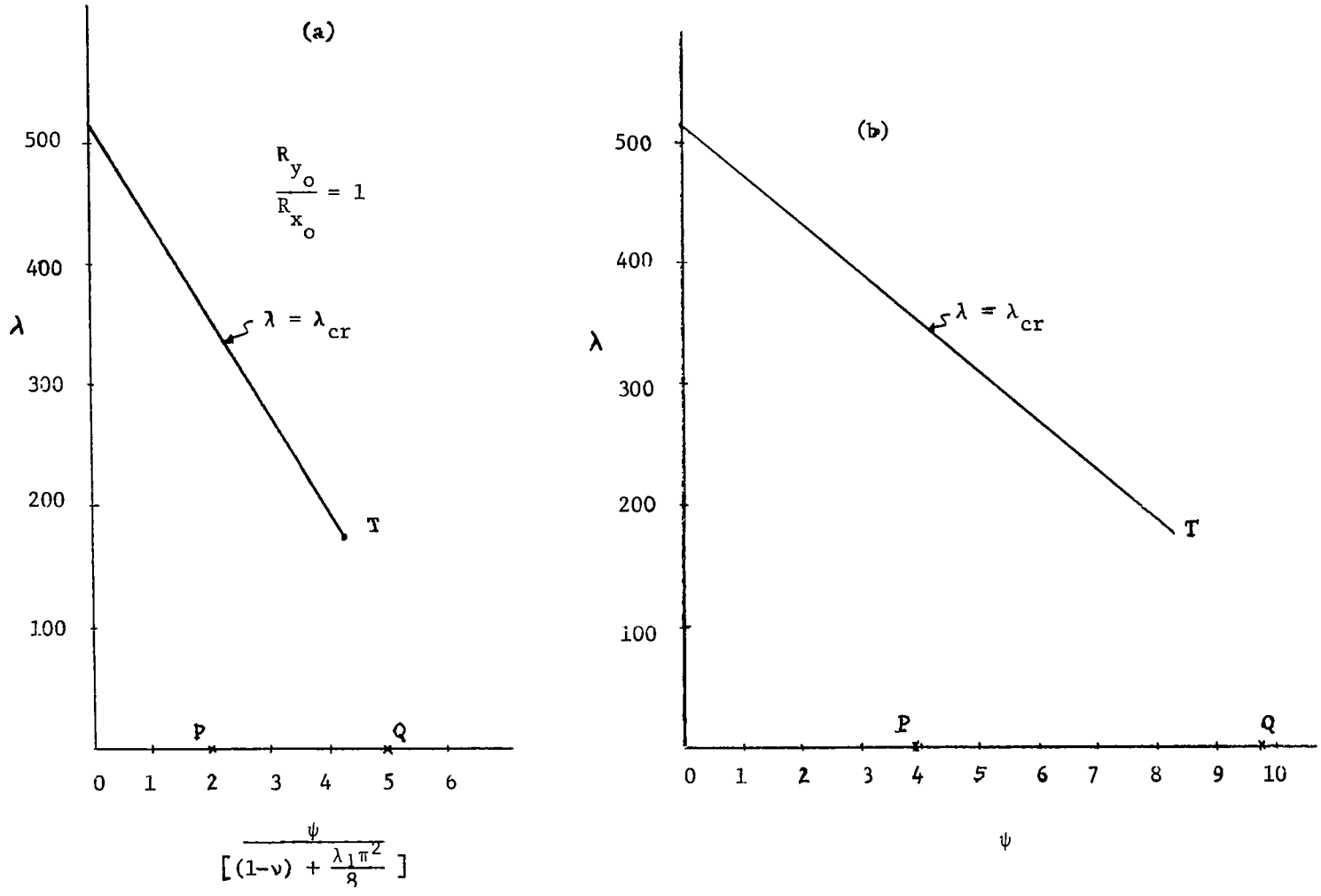

Figure 11. (a) Flutter Boundary (from ref. 1) for Uniform and Equal Biaxial Edge Loading of Unheated Square Plate. (b) Flutter Boundary for Case 3: Flexurally Rigid Stiffeners, Discontinuous Temperature Distribution.

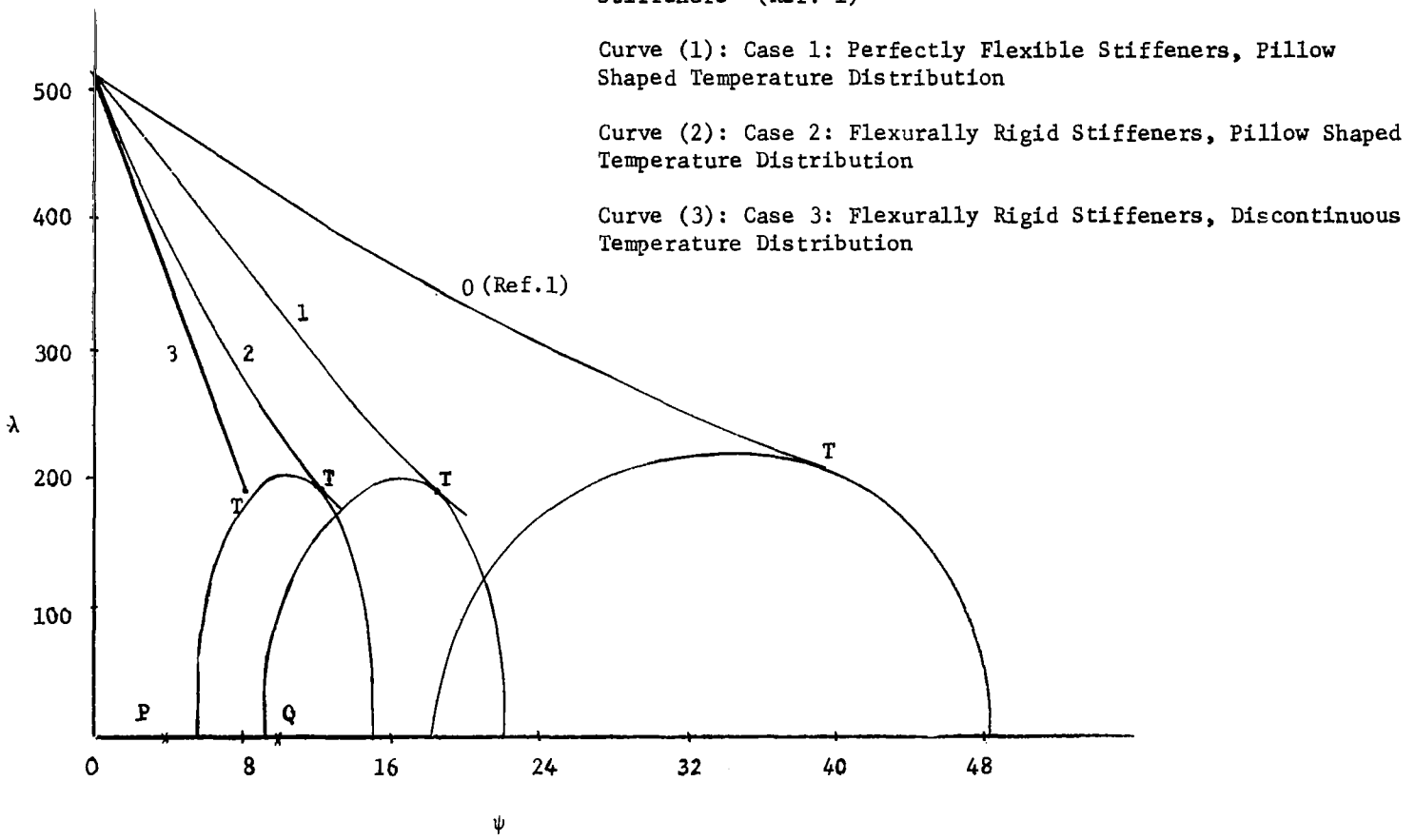

Figure 12. Summary of Present Results and Comparison with those of Reference 1.

REFERENCES

1. Schaeffer, Harry G., and Heard, Walter L. Jr., "Supersonic Flutter of a Thermally Stressed Flat Panel with Uniform Edge Loads." NASA TN D-3077, August 1965.
2. Libove, C., Panchal, D. and Dunn, F., "Plane-Stress Analysis of an Edge-Stiffened Rectangular Plate Subjected to Loads and Temperature Gradients." NASA TN D-2505, December, 1964.
3. Lin, Chuan-jui, and Libove, Charles, "Plane-Stress Analysis of an Edge-Stiffened Rectangular Plate Subjected to Boundary Loads, Boundary Displacements, and Temperature Gradients," NASA CR-864, August 1967.
4. Bohon, Herman L., and Dixon, Sidney C., "Some Recent Developments in Flutter of Flat Panels." J. Aircraft, Vol. 1, No. 5, Sept.-Oct. 1964, pp. 280-288.
5. Timoshenko, S. and Woinowsky-Krieger, S., "Theory of Plates and Shells." Second Edition. McGraw-Hill Book Company. p. 379.
6. Hedgepeth, John M., "Flutter of Rectangular Simply Supported Panels at High Supersonic Speeds." J. Aeron. Sci., Vol. 24, No. 8, August 1957, pp. 563-573, 586.
7. Bisplinghoff, Raymond L.,and Ashley, Holt, "Principles of Aeroelasticity." John Wiley and Sons Inc., C. 1962, pp. 60-62.
8. Francis, J. G. F., "The QR Transformation." Part I: The Computer Journal, Vol. 4, No. 5, pp. 265-271. Part II, ibid., January 1962, pp. 332-345.
9. Timoshenko, Stephen P., and Gere, James M., "Theory of Elastic Stability." Second Edition. McGraw-Hill Book Company. p. 356.

NASA-Langley, 1970 —— 32 CR-1574